

**The first study of the thermal and storage stability of arenediazonium triflates comparing to 4-nitrobenzenediazonium tosylate and tetrafluoroborate by calorimetric methods**

Alexander A. Bondarev<sup>1</sup>, Evgeny V. Naumov<sup>1</sup>, Assiya Zh. Kassanova<sup>2</sup>, Elena A. Krasnokutskaya<sup>3</sup>, Ksenia S. Stankevich<sup>3</sup>, Victor D. Filimonov<sup>3</sup>

<sup>1</sup>Department of Biomedicine, Altai State University, Barnaul, Russia, [alex\\_root@mail.ru](mailto:alex_root@mail.ru)

<sup>2</sup>S. Toraighyrov Pavlodar State University, Pavlodar, Kazakhstan

<sup>3</sup>The Kizhner Research Center, National Research Tomsk Polytechnic University, Tomsk, Russian Federation

## ABSTRACT

Herein, for the first time, using isothermal flow calorimetry and DSC/TGA, we have determined the thermal decomposition energies for the number of solid arenediazonium triflates comparing to 4-nitrobenzene tosylate and 4-nitrobenzentetrafluoroborate. The kinetics of thermal decomposition, activation energies, and half-lives of the studied diazonium salts were found. Using GC-MS and LC-MS, we have elucidated the products formed during thermolysis of the investigated diazonium salts. By DFT quantum chemical calculations at B3LYP/aug-cc-pVDZ level of theory we simulated the thermodynamics of decomposition reactions proceeding via substitution of diazonium group by corresponding nucleophiles. The applied method predicted the decomposition energies of all the studied compounds fairly precise, except for 2-nitrobenzene diazonium triflate. It has been found that 4-nitrobenzene diazonium triflate has an increased storage stability under normal conditions comparing to the corresponding tosylate and tetrafluoroborate. The experimental and theoretical results demonstrated that comparing to DSC/TGA, isothermal flow calorimetry more adequately reflects the energetics of the thermal decomposition of diazonium salts and their storage stability under normal conditions.

## INTRODUCTION

Aromatic diazonium salts (DSs) are versatile synthetic blocks widely used in fine organic synthesis and industry [1]. Beyond that, DSs have been increasingly applied in development of macro- and nanoscale composite materials due to their reactivity towards metal and non-metal surfaces [2].

Nevertheless, such disadvantages as a poor storage stability in solid state and a propensity to explosive decomposition upon heating, photoirradiation or mechanical stress [1a] limit the preparation and usage of DSs, especially, on an industrial scale.

Recently, we have synthesized arenediazonium tosylates  $\text{ArN}_2^+$   $\text{TsO}^-$  (ADTs) [3a] and trifluoromethane sulfonates  $\text{ArN}_2^+$   $\text{TfO}^-$  (ADTfs) [3b], that showed major advantages over traditional diazonium salts. While being surprisingly stable in solid state, they retained high reactivity in a vast array of diazonium chemistry reactions including the formation of aromatic iodides and bromides [3a, b, 4a-f], azides [3b, 4g] and boronic acids [3b], and Pd-catalyzed C-C-

cross-coupling [3b, 4h-j]. Additionally, it has been shown that ADTs can be successfully used for introducing <sup>19</sup>F isotope into the aromatic ring [5a], carrying out azo-coupling with ethyl-methyl acetoacetate [5b], substituting the diazonium group with the triethoxysilyl moiety [5c], and covalently grafting aromatic groups to carbonized metal nanoparticles [5d] and graphene [5e].

The thermal decomposition energies of some ADTs and ADTfs, determined by DSC/TGA, in most cases were found to be below 800 J/g. Therefore, according to the safety criteria of the United Nations Economic Commission for Europe (UNECE) they can be referred as compounds that can be transported safely [6]. However, the products of their thermal decomposition have not been studied and remain unknown. Moreover, DSC/TGA provides information about thermal decomposition energy at elevated and high temperatures and does not reflect decomposition processes taking place under normal conditions. To comprehensively assess the possibility of safe use of ADTs and ADTfs in the laboratory and on an industrial scale, it is necessary to determine reliable quantitative characteristics of their storage stability in a solid state and thermal decomposition energies. Such evaluations should be done using various methods and comparing to other types of DSs.

Noteworthy, the DS decomposition in solution has been extensively investigated for a long time (see, for example, [1a,g]), whereas not many studies cover stability and safety of DSs in the solid state. The paucity of quantitative data describing the decomposition of solid DSs reflects the lack of reliable generally accepted procedures for measuring the above-mentioned properties.

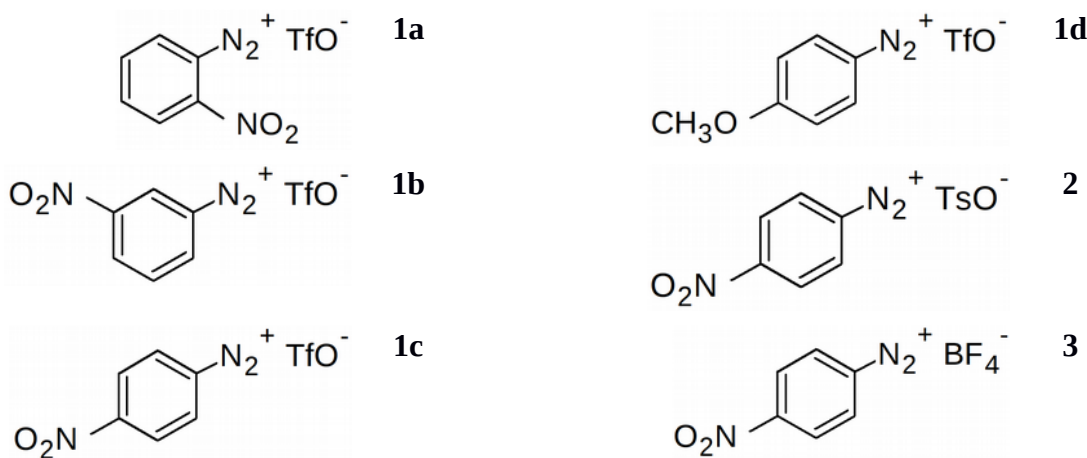
A comparative study of the stability of the solid DSs (chlorides, tetrachlorozincates and tetrafluoroborates) was reported in [7a,c], however the decomposition products were not given. The investigation of the thermal decomposition of <sup>14</sup>N- and <sup>15</sup>N-substituted arenediazonium chlorides and tetrafluoroborates has shown that isotope effect is insensitive to the nature and position of substituents in the aromatic ring and the nature of the counterion [7b]. The stability test of arenediazonium chlorides has demonstrated that the sensitivity to detonation decreases from *ortho*-, through *meta*-, to *para*- substitution [7a]. It was shown that the nature of the substituent in the aromatic nucleus has a pronounced effect on DS stability as the nitro derivatives were significantly more sensitive to impact than the chlorine derivatives. The decrease in detonation sensitivity with an increase in molecular weight was observed, which was associated with a decrease in the specific value of the energy released per unit mass. The authors noted that the detonation sensitivity of DSs depends on many factors such as the size and shape of the crystals, as well as the presence of impurities. No correlation between detonation sensitivity and thermal stability was found [7a]. The values of the thermal decomposition energies of some ADTs and ADTfs, determined by DSC/TGA, do not correlate with the structural features of the diazonium cation or the nature of counterion [3a, b, g]. The commonly occurred term “the storage stability of DS” has not yet been described quantitatively. To address this issue, in most cases the ability of DSs to be stored without changes for a certain time is indicated. Besides, to the best of our knowledge, up to the present, there are no theoretical methods for predicting the energies of thermal decomposition of DSs based on their chemical structure.

Our work aims to comprehensively address the challenges associated with the thermal and storage stability assessment of DSs. To achieve that, we for the first time have studied the kinetics and thermodynamics of thermal decomposition of arenediazonium triflates **1a-d** comparing to 4-nitrobenzenediazonium tosylate **2** and tetrafluoroborate **3** by DSC/TGA and isothermal flow calorimetry. Additionally, we have endeavored to develop the criteria for the evaluation of the storage stability of an array of diazonium salts with various counterions and substituents. The electron-withdrawing nitro group and the electron-donating methoxy group were chosen as substituents in the aromatic core of ADTfs **1a-d** for the following reasons. First, according to [7a], diazonium salts with  $\text{NO}_2^-$  moieties are the most explosive, therefore they represent the highest threshold of these properties. Secondly, DSs with  $\text{NO}_2^-$  and  $\text{MeO}^-$  substituents in the aromatic ring differ sharply in their properties [3a, b], i.e. these two examples should cover the widest range of properties studied.

We also aimed to determine the possibility to apply DFT quantum chemical calculations for the theoretical evaluation of the DS thermal decomposition and clarification of its mechanism. To the best of our knowledge, DFT methods have not been previously used for these purposes. To investigate the mechanism, a GC-MS and LC-MS study of the decomposition products of DSs **1a-d**, **2**, **3** was carried out. The obtained results are valuable for both applied and theoretical field of diazonium chemistry. On the one hand, they allow to assess the stability, capabilities and limitations of DSs for industrial use. On the other hand, they provide the better understanding of the mechanisms of DS thermal decomposition and allow to establish the structure-stability relationship.

## MATERIALS AND METHODS

Arenediazonium triflates **1a-d** and 4-nitrobenzenediazonium tosylate **2** were synthesized according to the procedure described previously [3a,b]. 4-Nitrobenzenediazonium tetrafluoroborate **3** was purchased from Aldrich {Was it Aldrich or Sigma or Merk? I know its kinda complicated now})(CAS № 456-27-9).



**Scheme 1.** {Was it Aldrich or Sigma or Merk? I know its kinda complicated now}) The structures of arenediazonium triflates **1a-d**, 4-nitrobenzenediazonium tosylate **2** and 4-nitrobenzenediazonium tetrafluoroborate **3**

The DSC/TGA runs were made in argon atmosphere using open sample pans on Q600 SDT instrument (TA Instruments). Heat flow was measured under isothermal conditions in nitrogen atmosphere using TAM III microcalorimeter (TA Instruments). The typical sample size was 10 mg. {I suggest to mention the following parameters: a heating rate, temperature range, gas purge flow} Sample was put in a glass beaker placed in a standard calorimeter ampoule made from *Hastelloy* with a volume of 1 mL. The beaker {Am I right that you evacuate the beaker that is placed into the ampoule?} was evacuated and then purged with nitrogen, argon or air depending on experimental conditions. The acquired experimental curves were approximated using the model of an autocatalytic process and the Arrhenius equation {I have found the full text of the paper you referring to, so I am not entirely sure if I am correct here.} according to the recommendations for a calorimetric study of the safety of energetic materials [8]. The experimental data were processed using TAM Assistant Software v1.3.0.153. Gnuplot 4.5 [9a] and R Statistics v3.3.3 [9b] were used for mathematical processing, statistical analysis, and dependencies building.

The DS decomposition products were studied by GC-MS on an Agilent 7890A\5975C instrument. The typical sample size was 50 mg. Samples were heated in a thermostat at 85 ° C for 14 days. Then an aqueous solution of KI was added to the sample to convert the undecomposed diazonium salts into the corresponding volatile aryl iodides [3a, b], the products were extracted with ethyl acetate and organic layer was filtered through a silica pad. The obtained ethyl acetate extracts were then analyzed by GC-MS.

All LC-MS experiments were carried out on a high-resolution time-of-flight mass spectrometer Agilent LC-1260 MS QTOF 6530 equipped with electrospray ionization source (ESI) and atmospheric pressure chemical ionization source (APCI). A chromatographic method was developed using a Zorbax Eclipse Plus column (C18, 2.1x50 mm, 1.8 micron). The following gradient elution with water as “A” and acetonitrile as “B” was used at a flow rate of 0.25 mL/min: 0-40 min, 0% B → 100% B followed by isocratic elution with B for 20 min. Потенциал на фрагменторе 150 В. Напряжение на капилляре 3500 В. Энергия столкновений MSMS - 20 эВ. {Are those the parameters of ESI or APCI? Did you use both sources for your experiments? What is “fragmentor”? Is it like the part of the device where compound is ionized?} For the LS-MS experiments, the DS decomposition products were dissolved in a water:acetonitrile mixture (1:1 v/v) at a concentration of 1 mg/mL. The volume of sample injected was 5 µL. Acquired LS-MS spectra were processed using the OpenMS 2.0 software package [10a,b].

For the theoretical study of suggested DS decomposition routes the quantum-chemical calculations were performed using Kohn-Sham density functional theory (DFT), global-hybrid GGA functional B3LYP and aug-cc-pVDZ basis set in Gaussian 09 software package [11]. At the first step, the geometry of all molecules participating in the reactions was optimized. To prove the nature of the stationary points, the harmonic frequency calculations were done. Thereafter, the vibrational frequencies and thermodynamic corrections {Is it correct?} were calculated at normal conditions (25 ° C, 1 atm) and at temperatures used for isothermal decomposition experiment (75, 80 and 85 ° C). {You haven't mentioned those temperatures in above passages. Is it temperatures used for decomposition products study?}

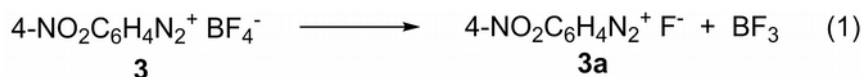
## RESULTS AND DISCUSSION

### DSC/TGA results

Our study of the thermal and storage stability of arenediazonium triflates **1a-d**, 4-nitrobenzenediazonium tosylate **2** and tetrafluoroborate **3** has begun from collecting DCS/TGA data. Fig. 1-6 show DSC/TGA curves of thermal decomposition of DSs **1-3**. It can be seen that upon heating all the investigated DSs decompose with energy and weight loss. The temperatures and decomposition energies are summarized in Table 1.

For the DSs **1a,b,d**, **3** additional low-temperature endothermic effects are observed in the temperature range close to their melting point, whereas DSs **1c**, **2** decomposed only exothermically (Fig. 1-6, Table 1). Note that DS **2** decomposes giving two exothermic peaks (Fig. 5). The first one at 69.37 ° C is characterized by a small amount of heat released (24.47 J/g), while for the second one, located at 146.6 ° C, the heat release of 323.0 J/g is observed. In the case of DSs **1a**, **1b**, **1d** the endothermic peaks are not accompanied by a weight loss and are probably associated with the destruction of the crystal lattice during melting.

The weight loss upon heating DS **3** in the endothermic process, starting at 33.7 ° C is 28.5%, which corresponds exactly to the elimination of volatile BF<sub>3</sub> (28.6%) according to reaction (1):



This indicates that 4-nitrobenzene diazonium fluoride **3a** should undergo further decomposition at 146.5 ° C.

The major weight loss upon heating of DSs **1-3** occurs in exothermic processes, which is clearly associated with the formation of volatile decomposition products (Fig. 1-6).

Table 1. Temperatures and decomposition energies of diazonium salts **1-3** according to DSC\TGA experiments data.

Diazonium salts	Endothermic process		Exothermic process	
	T, ° C	ΔH, J/g (kJ/mol)	T, ° C	ΔH, J/g (kJ/mol)
2-NO <sub>2</sub> C <sub>6</sub> H <sub>4</sub> N <sub>2</sub> <sup>+</sup> TfO <sup>-</sup> <b>1a</b>	104.1	73.49 (21.98)	143.3	-753.4 (-225.3)
3-NO <sub>2</sub> C <sub>6</sub> H <sub>4</sub> N <sub>2</sub> <sup>+</sup> TfO <sup>-</sup> <b>1b</b>	102.5	43.6 (10.04)	111.2	-840.4 (-251.3)
4-NO <sub>2</sub> C <sub>6</sub> H <sub>4</sub> N <sub>2</sub> <sup>+</sup> TfO <sup>-</sup> <b>1c</b>	-	-	116.4	-219.9 (-65.7)
4-MeOC <sub>6</sub> H <sub>4</sub> N <sub>2</sub> <sup>+</sup> TfO <sup>-</sup> <b>1d</b>	88.4	102.2 (29.05)	136.6	-328.9 (-93.5)
4-NO <sub>2</sub> C <sub>6</sub> H <sub>4</sub> N <sub>2</sub> <sup>+</sup> TsO <sup>-</sup> <b>2</b>	-	-	69.37 146.6	-24.47 (-7.8) -323.0 (-103.7)
4-NO <sub>2</sub> C <sub>6</sub> H <sub>4</sub> N <sub>2</sub> <sup>+</sup> BF <sub>4</sub> <sup>-</sup> <b>3</b>	33.7	617.3 (146.3)	146.5	-229.2 (-54.3)

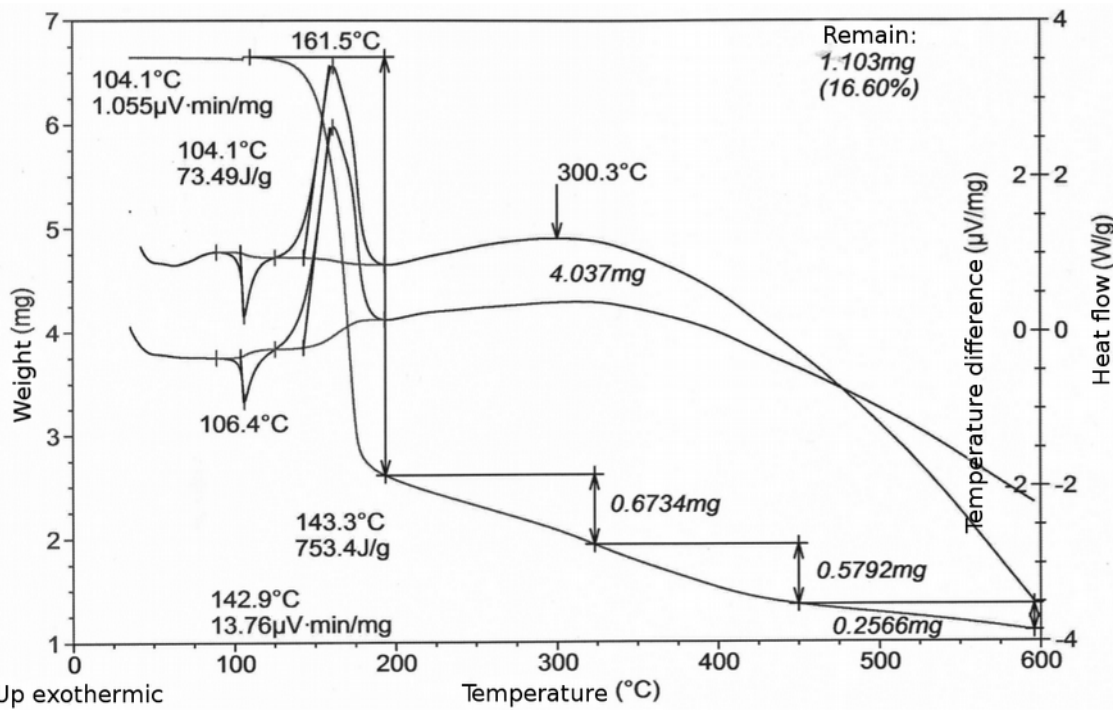


Figure 1. DSC/TGA thermograms of thermal decomposition of DS  $2\text{-NO}_2\text{C}_6\text{H}_4\text{N}_2^+$   $\text{TfO}^-$  **1a**

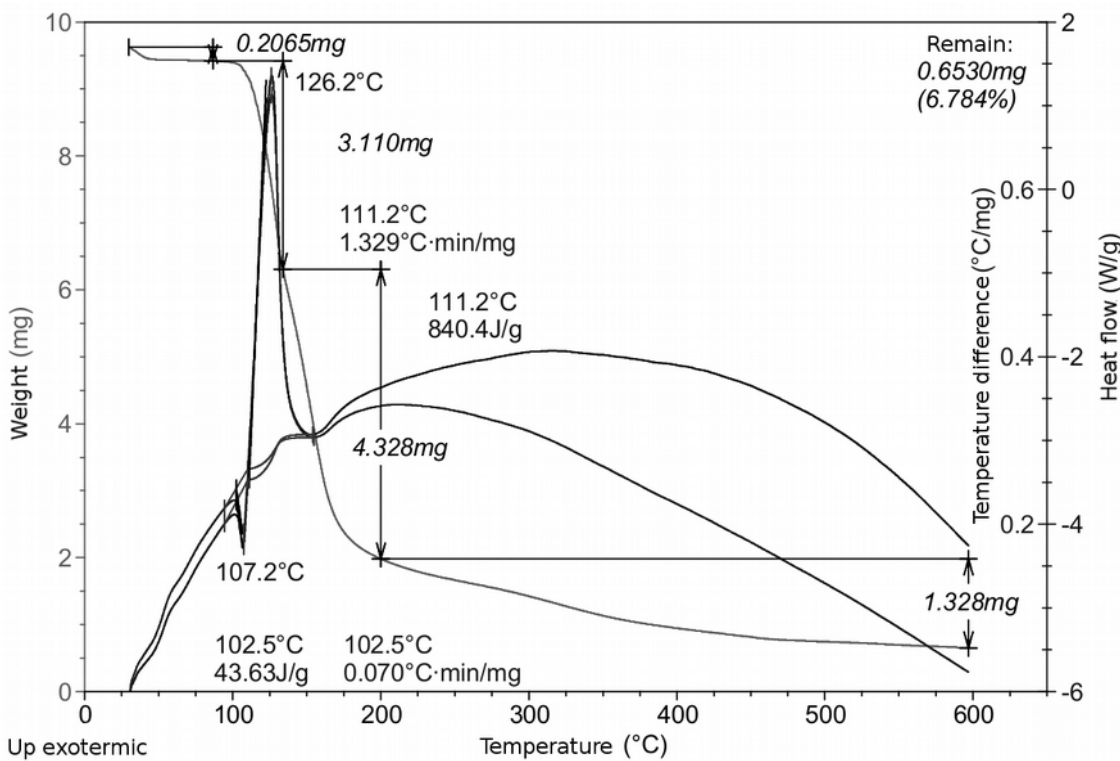


Figure 2. DSC/TGA thermograms of thermal decomposition of  $3\text{-NO}_2\text{C}_6\text{H}_4\text{N}_2^+$   $\text{TfO}^-$  **1b**

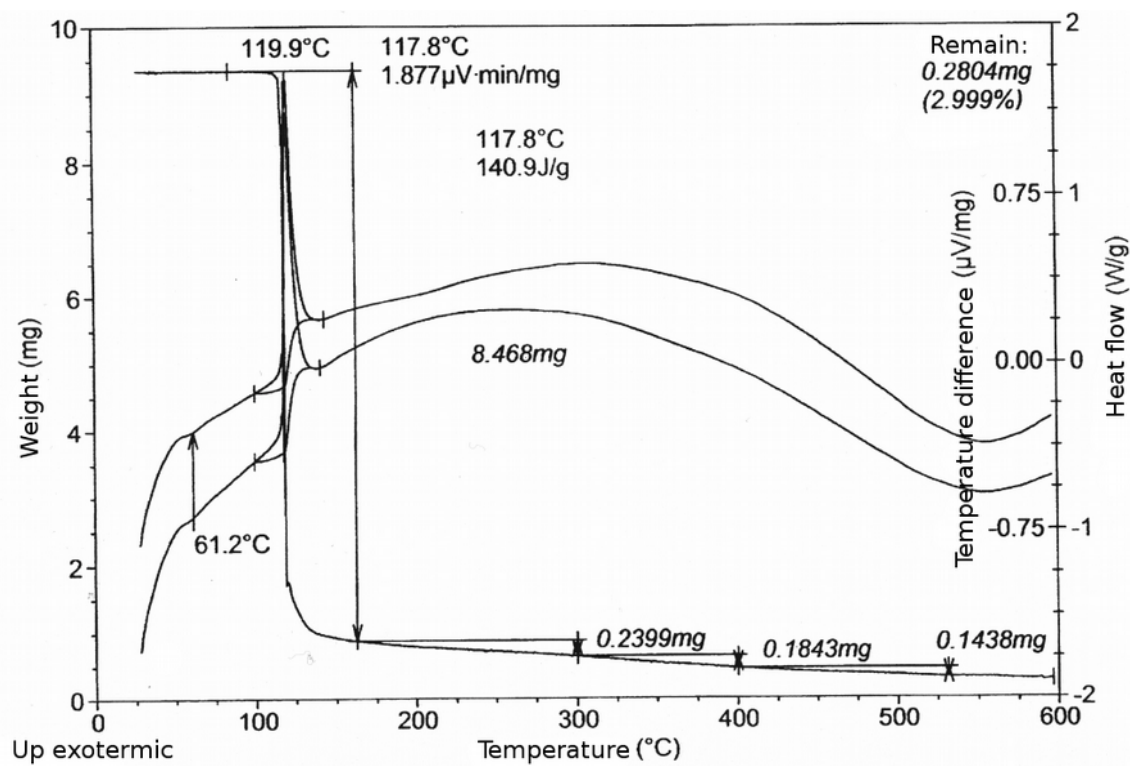


Figure 3. DSC/TGA thermograms of thermal decomposition of  $4\text{-NO}_2\text{C}_6\text{H}_4\text{N}_2^+\text{TfO}^-$  **1c**

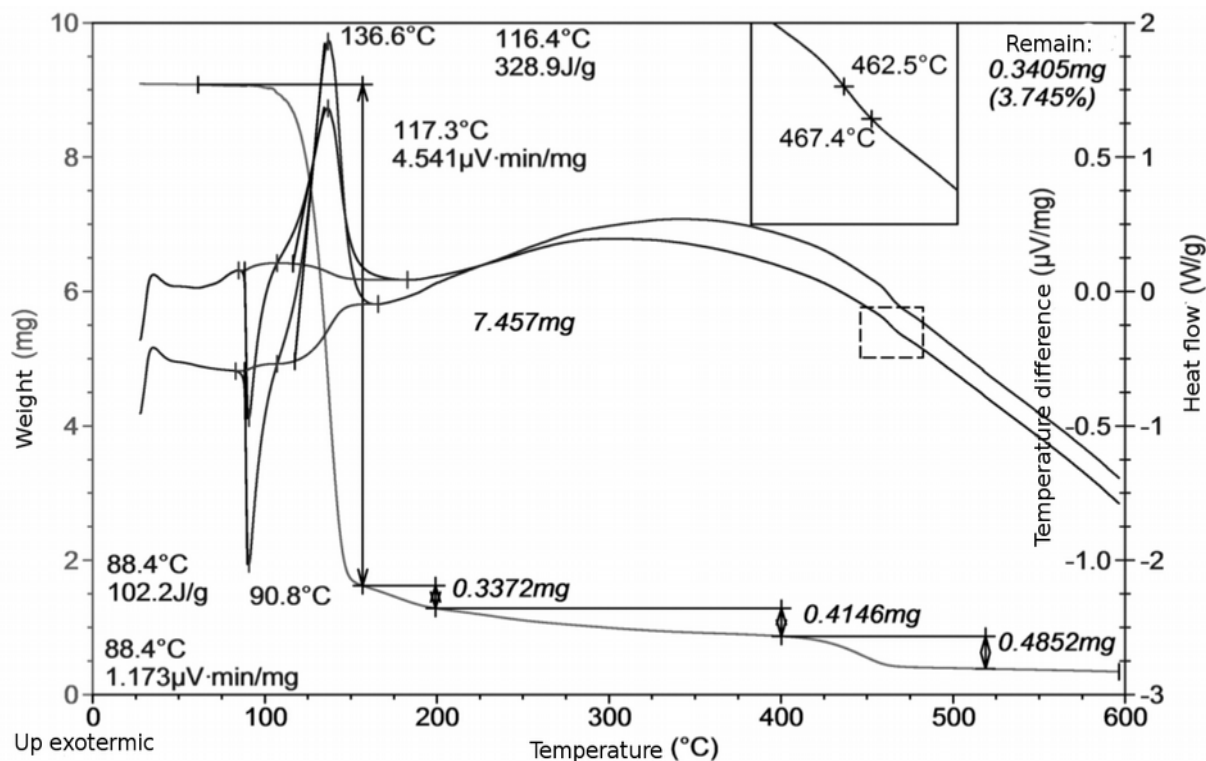


Figure 4. DSC/TGA thermograms of thermal decomposition of  $4\text{-MeOC}_6\text{H}_4\text{N}_2^+\text{TfO}^-$  **1d**

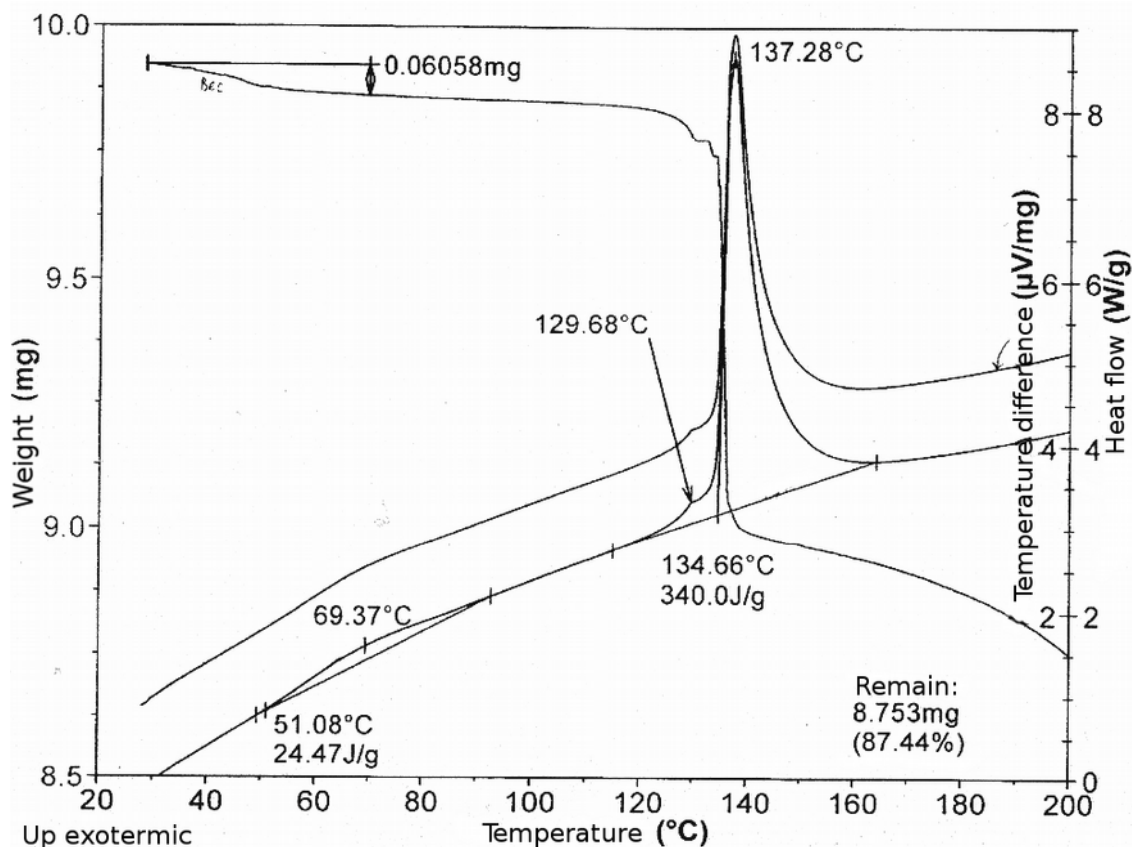


Figure 5. DSC/TGA thermograms of thermal decomposition of  $4\text{-NO}_2\text{C}_6\text{H}_4\text{N}_2^+\text{TsO}^-$  2 c

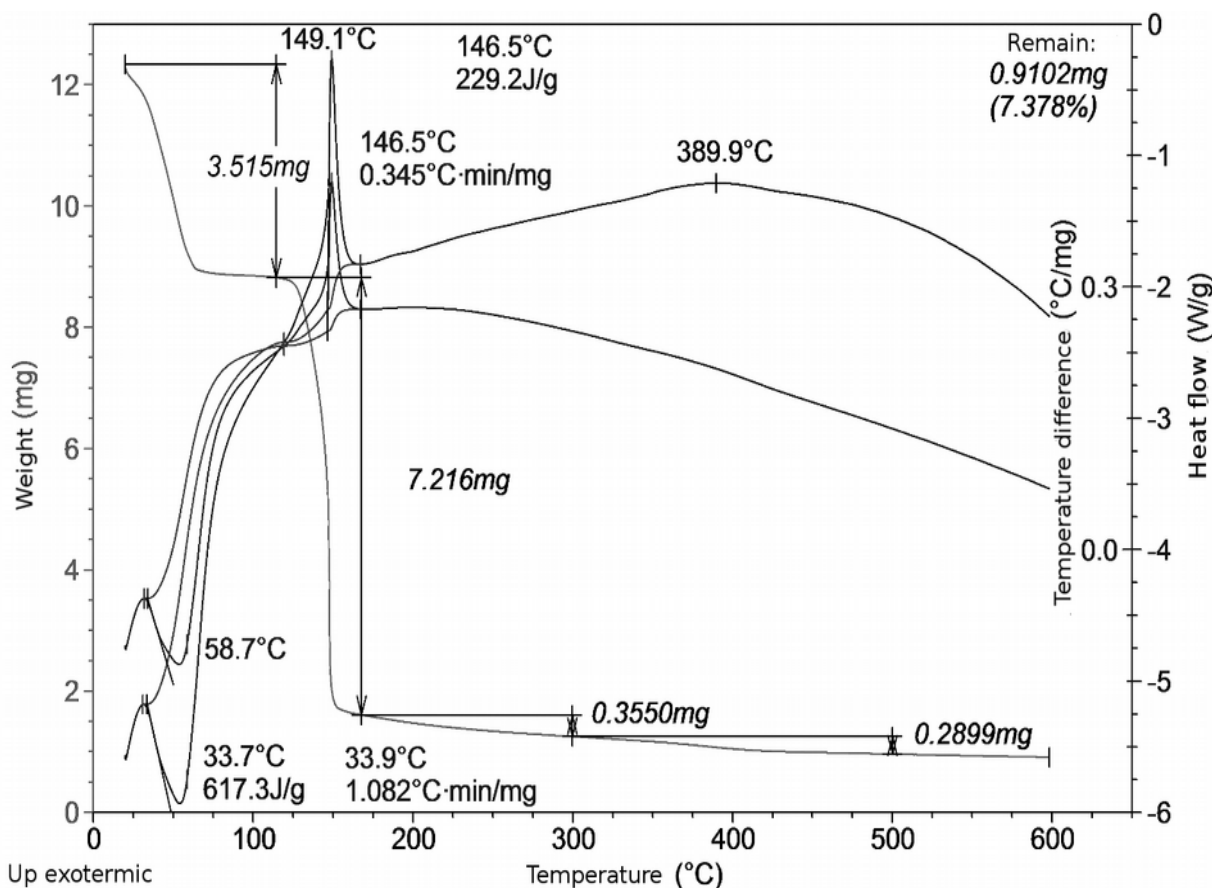


Figure 6. DSC/TGA thermograms of thermal decomposition of  $4\text{-NO}_2\text{C}_6\text{H}_4\text{N}_2^+\text{BF}_4^-$  3

The exothermic effects  $\Delta H_{\text{exotherm}}$  of DSs **1-3** thermal decomposition are the most important for the DS safety evaluation. As can be seen from Table 1, these effects strongly depend on the nature and position of the substituent in the benzene ring and partly on the nature of counterions. Among salts **1a-d** with a triflate counterion, the energy release during decomposition is the highest for 3-nitro-derivative **1b** and decreases noticeably in the row **1b > 1a > 1d > 1c**. Among DSs having the same 4-nitrobenzene diazonium cation and different counterions, the energy release decreases in the row **2c > 1c ≈ 3**. Therefore, the highest heat release is observed for DS with a TsO<sup>-</sup> counterion. However, a change in the counterion nature affects exothermic decomposition process substantially less than the position and type of substituents in the benzene ring.

### Isothermal flow calorimetry results

With DSC/TGA data in our hands we moved on to isothermal flow calorimetry analysis of DSs studied. As the stability of DS could be affected by the presence of impurities, which are often cannot be controlled by conventional analytical methods [1a, 7a], we first decided to evaluate the reproducibility of thermal decomposition parameters measured. To do that we took samples of ADTS **2** from three synthetic batches obtained under identical conditions (samples 1-3) and samples of ADTS **2** purified by single and double precipitation of sample 3 from acetic acid/ether solutions (reprecipitation 1 and 2). During the isothermal decomposition the following parameters have been determined: the integral enthalpy, initial and maximum heat flows, decomposition rate constants, and initial product concentrations approximated by Equation 2. Additionally, we have varied the purged gas and studied sample decomposition in air, argon and nitrogen atmosphere. The results show that the collected data are consistent, and the results do not depend statistically significantly on the degree of sample purification. Even though there is a slight tendency to the reduction of the initial heat flow depending on the number of reprecipitations, the differences between the first and second reprecipitation are minimal. No qualitative and statistically significant differences were observed when decomposition was conducted in air, argon and nitrogen atmosphere. The average statistical deviation (RMD) for the rate constants (according to equation 2) and the enthalpy was 5%. Therefore, the further isothermal flow calorimetry experiments were carried out in a nitrogen atmosphere and after a single reprecipitation of the initial DS.

Table 2. The reproducibility of the DS **2** thermal decomposition parameters measured at 85 ° C depending on synthetic batch and a number of reprecipitations (k – rate constant,  $C_0$  — initial product concentration according to equation 2,  $\Delta H$  - integral enthalpy,  $P_0$  — initial heat flow).

Sample	$k, \text{g}\cdot\text{mol}^{-1}\cdot\text{c}^{-1}$	$\Delta H, \text{kJ}\cdot\text{mol}^{-1}$	$P_0, \text{mW/g}$
Sample 1 Nitrogen (reprecipitation 1)	$0.0875 \pm 0.0117$	$234.2 \pm 3.0$	$31.2 \pm 8.1$
Sample 2 Nitrogen, (source, reprecipitation 1)	$0.0825 \pm 0.0119$	$243.6 \pm 20.7$	$12.7 \pm 3.5$
Sample 3 Nitrogen, (source, reprecipitation 1)	$0.0848 \pm 0.0091$	$235.5 \pm 7.0$	$10.1 \pm 3.5$
Sample 3 Air, reprecipitation 2	$0.0862 \pm 0.0107$	$229.0 \pm 28.9$	$8.7 \pm 8.5$
Sample 3 Argon, reprecipitation 2	$0.1002 \pm 0.0113$	$242.3 \pm 8.0$	$12.8 \pm 2.4$

Sample 2, 3 Nitrogen, (source, reprecipitation 1, 2)	$0.0838 \pm 0.0059$	$238.9 \pm 7.8$	$11.2 \pm 2.3$
Sample 4 Nitrogen, source	$0.0832 \pm 0.0109$	$241.7 \pm 16.2$	$12.0 \pm 2.0$
Sample 4 Nitrogen, reprecipitation 1	$0.0838 \pm 0.0158$	$235.1 \pm 17.9$	$10.2 \pm 6.3$
Sample 4 Nitrogen, reprecipitation 2	$0.0931 \pm 0.0071$	$238.1 \pm 6.8$	$11.3 \pm 2.3$
<b>General statistics</b>	<b><math>0.0882 \pm 0.0045</math></b>	<b><math>237.7 \pm 4.6</math></b>	<b><math>13.8 \pm 3.3</math></b>

Table 1 and Fig. 7-10 show the results of isothermal decomposition of DSs **1-3** at 75 °C, 80 °C, and 85 °C. At 75 °C, the maximum heat flow values obtained for the 4-nitrobenzenediazonium salts **1c**, **2**, **3** almost do not depend on the counterion nature. However, it can be noted that the P curve acquired during DS **1c** decomposition is much steeper. Additionally, the  $P_{\max}$  values obtained for this DS at 80 and 85 °C are significantly higher than those for DS **2** and **3**. The  $P_{\max}$  values found for 4-methoxybenzenediazonium triflate **1d** are noticeably smaller comparing to 4-nitrobenzenediazonium triflate **1c**. Among the nitrobenzenediazonium triflates **1a-c**, the maximum heat flow decreases from *para*- **1c**, through *meta*- **1b**, to *ortho*- **1a** substitution. The values of  $P_{\max}$  are important not only for mathematical modeling of the reaction kinetics, but also for quantitative description of the compound safety that is essential for practical application.

Table 3. Integral enthalpy and maximum heat flow values found during isothermal decomposition of diazonium salts **1-3** ( $\Delta H$  – integral enthalpy,  $P_{\max}$  – maximum heat flow value).

Diazonium salt	$\Delta H$ , kJ/mol			$P_{\max}$ , mW/g		
	75°	80°	85°	75°	80°	85°
2-NO <sub>2</sub> C <sub>6</sub> H <sub>4</sub> N <sub>2</sub> <sup>+</sup> TfO <sup>-</sup> ( <b>1a</b> )	414.0	386.0	396.0	0.705	1.49	2.33
3-NO <sub>2</sub> C <sub>6</sub> H <sub>4</sub> N <sub>2</sub> <sup>+</sup> TfO <sup>-</sup> ( <b>1b</b> )	227.9	230.0	225.4	6.57	14.15	28.8
4-NO <sub>2</sub> C <sub>6</sub> H <sub>4</sub> N <sub>2</sub> <sup>+</sup> TfO <sup>-</sup> ( <b>1c</b> )	200.0	235.1	250.0	20.12	47.89	101.5
4-MeOC <sub>6</sub> H <sub>4</sub> N <sub>2</sub> <sup>+</sup> TfO <sup>-</sup> ( <b>1d</b> )	183.1	183.2	106.0	1.34	2.97	5.37
4-NO <sub>2</sub> C <sub>6</sub> H <sub>4</sub> N <sub>2</sub> <sup>+</sup> TsO <sup>-</sup> ( <b>2</b> )	253.0	232.4	231.0	21.10	34.82	64.60
4-NO <sub>2</sub> C <sub>6</sub> H <sub>4</sub> N <sub>2</sub> <sup>+</sup> BF <sub>4</sub> <sup>-</sup> ( <b>3</b> )	173.0	156.0	147.0	20.02	31.63	66.87

To investigate the kinetics of isothermal decomposition (Fig. 7-10), we approximated the experimental heat flow curves with kinetic equation for autocatalytic reactions (2) that qualitatively describes the heat flow over time dependency. The following main parameters were determined:  $k$  - rate constant, and  $P_0$ ,  $P_{\max}$  - values of the initial and maximum heat flows in the autocatalytic reaction equation 2. Table 4 shows calculated kinetic parameters found as result of approximation of

the experimental heat flow curves of DSs **1a-1d**, **2**, **3**. The following kinetic equation for autocatalytic reactions that was applied:  $a A \rightarrow c C$

$$\frac{dC}{dt} = k \cdot \left( A_0 - \frac{a}{c} \cdot (C - C_0) \right) \cdot C_0$$

$$P = \frac{dC}{dt} \cdot \Delta H; \quad P_0 = k \cdot A_0 \cdot C_0 \cdot \Delta H; \quad (2)$$

(where  $A_0$  – initial DS concentration, which for solid-phase reactions is measured in  $\text{mol/g}$  units;  $C_0$ ,  $C$  – initial and current concentrations of products, [ $\text{mol/g}$ ];  $k$  – rate constant;  $a$ ,  $c$  – stoichiometric coefficients, for the processes studied  $a/c=1$ ;  $P$ ,  $P_0$  – current and initial heat flow)

Figure 7 shows the experimental heat flow curves describing the isothermal decomposition of DSs **1c**, **2** and **3** at  $85^\circ\text{C}$ . As can be seen, the half-life of DSs depends on the counterion: for tetrafluoroborate **3** it is 2.1 h, for triflate **1c** – 4.5h, and for tosylate **2** – 6h.

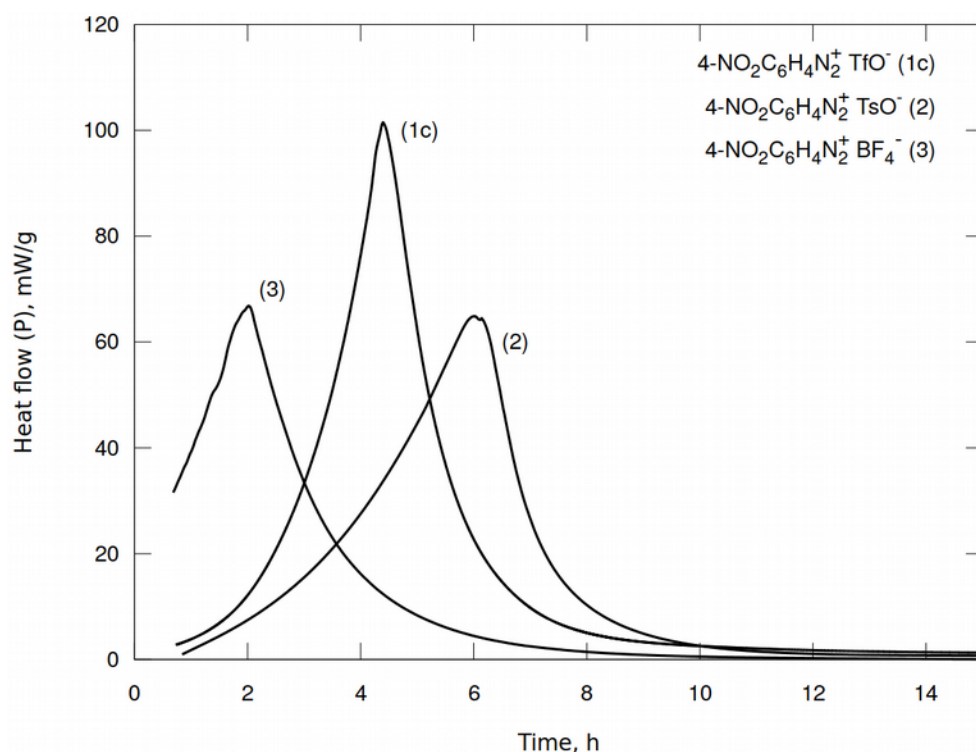


Figure 7. The heat flow ( $P$ ) during isothermal decomposition of nitrobenzenediazonium salts: tetrafluoroborate **3**, tosylate **2**, and triflate **1c** at  $85^\circ\text{C}$ .

The experimental heat flow curves describing the isothermal decomposition of salt **1a** are more complex and, therefore, differ from the curve characteristic for the autocatalytic process. At the initial stage, a decrease in the heat flow is observed, which is associated with a higher rate of endothermic process. Then, the heat flow is increased indicating the predominance of the exothermic process. The presence of the endothermic process is consistent with the DSC/TGA data

(Table 1). To describe the kinetics of this reactions, we used the model of two sequential and two parallel autocatalytic processes. The deconvolution results are given in detail in Supporting (1s). Table 4 shows the parameters of the heat flow kinetics calculated when isothermal decomposition reaction is approximated by a single autocatalytic process corresponding to the main exothermic stage. This stage is the most important as it determines the main characteristics of safety and stability of DSs.

Table 4. Kinetic parameters of the isothermal decomposition of DSs **1-3** ( $P_0$  – initial heat flow value,  $k$  – rate constant calculated according to the equation 2).

Diazonium salt	$P_0$ , mW			$k$ , g mol <sup>-1</sup> c <sup>-1</sup>		
	75°	80°	85°	75°	80°	85°
2-NO <sub>2</sub> C <sub>6</sub> H <sub>4</sub> N <sub>2</sub> <sup>+</sup> TfO <sup>-</sup> <b>1a</b>	4.06	8.82	14.7	0.00026	0.00055	0.00076
3-NO <sub>2</sub> C <sub>6</sub> H <sub>4</sub> N <sub>2</sub> <sup>+</sup> TfO <sup>-</sup> <b>1b</b>	0.0097	1.10	4.46	0.00912	0.01958	0.0429
4-NO <sub>2</sub> C <sub>6</sub> H <sub>4</sub> N <sub>2</sub> <sup>+</sup> TfO <sup>-</sup> <b>1c</b>	0.900	1.311	4.84	0.0316	0.0630	0.1599
4-MeOC <sub>6</sub> H <sub>4</sub> N <sub>2</sub> <sup>+</sup> TfO <sup>-</sup> <b>1d</b>	1.477	3.200	11.38	0.0021	0.0044	0.0128
4-NO <sub>2</sub> C <sub>6</sub> H <sub>4</sub> N <sub>2</sub> <sup>+</sup> TsO <sup>-</sup> <b>2</b>	1.957	2.745	4.152	0.0289	0.0539	0.1030
4-NO <sub>2</sub> C <sub>6</sub> H <sub>4</sub> N <sub>2</sub> <sup>+</sup> BF <sub>4</sub> <sup>-</sup> <b>3</b>	39.241	89.598	180.42	0.0186	0.0344	0.0721

The half-life of 4-nitrophenyldiazonium triflate **1c** is significantly less than the half-life of 4-methoxyphenyldiazonium triflate **1d**: the values found are 4 h and 10 h, respectively. At the same time, the heat flow observed during decomposition of 4-nitrophenyldiazonium triflate **1c** is much higher than that of 4-methoxyphenyldiazonium triflate **1d** (Fig. 8): 101.5 mW/g for **1c** versus 5.37 mW/g for **1d** (Fig.8).

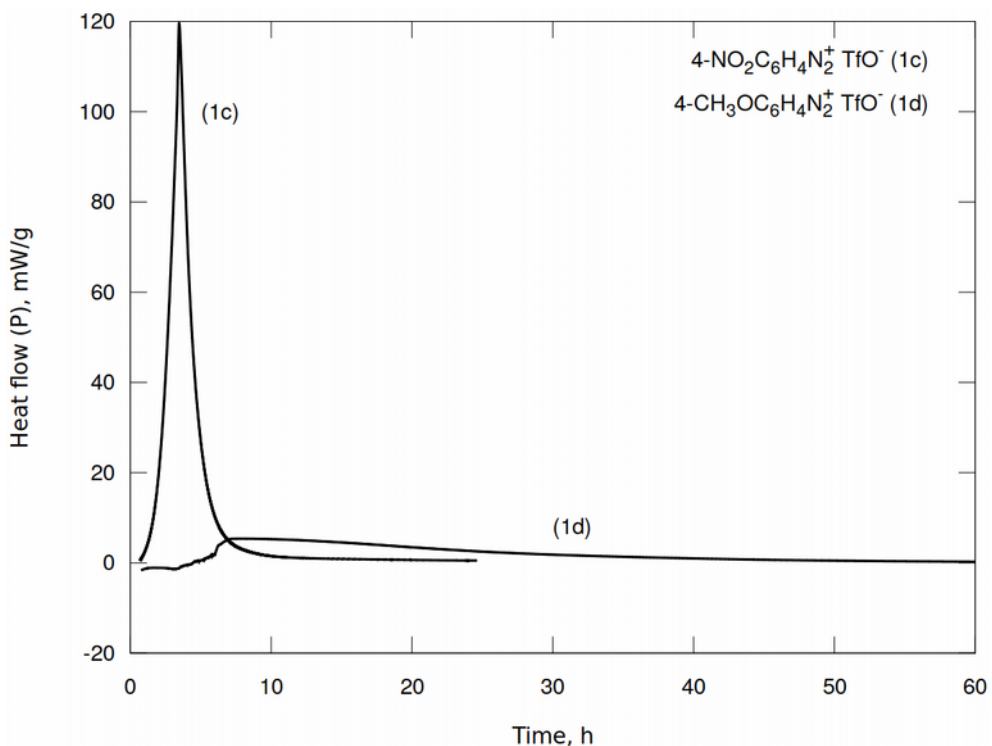


Figure 8. The heat flow (P) during isothermal decomposition of 4-nitrobenzenediazonium **1c** and 4-methoxybenzenediazonium **1d** triflates at 85 °C.

The substitution pattern in aromatic ring has a pronounced effect on the DS stability. Among DS with triflate counterion, the longest half-life time at 85° C has *ortho*- derivative **1a** (45 h). The *meta*- derivative **1b** is less stable (11 h) and *para*- derivative **1c** is the least stable (5 h). The maximum heat flow values follow the opposite pattern and decrease in a row **1c** > **1b** > **1a**. The results discussed are presented in Tables 3 and 4 and Fig.9.

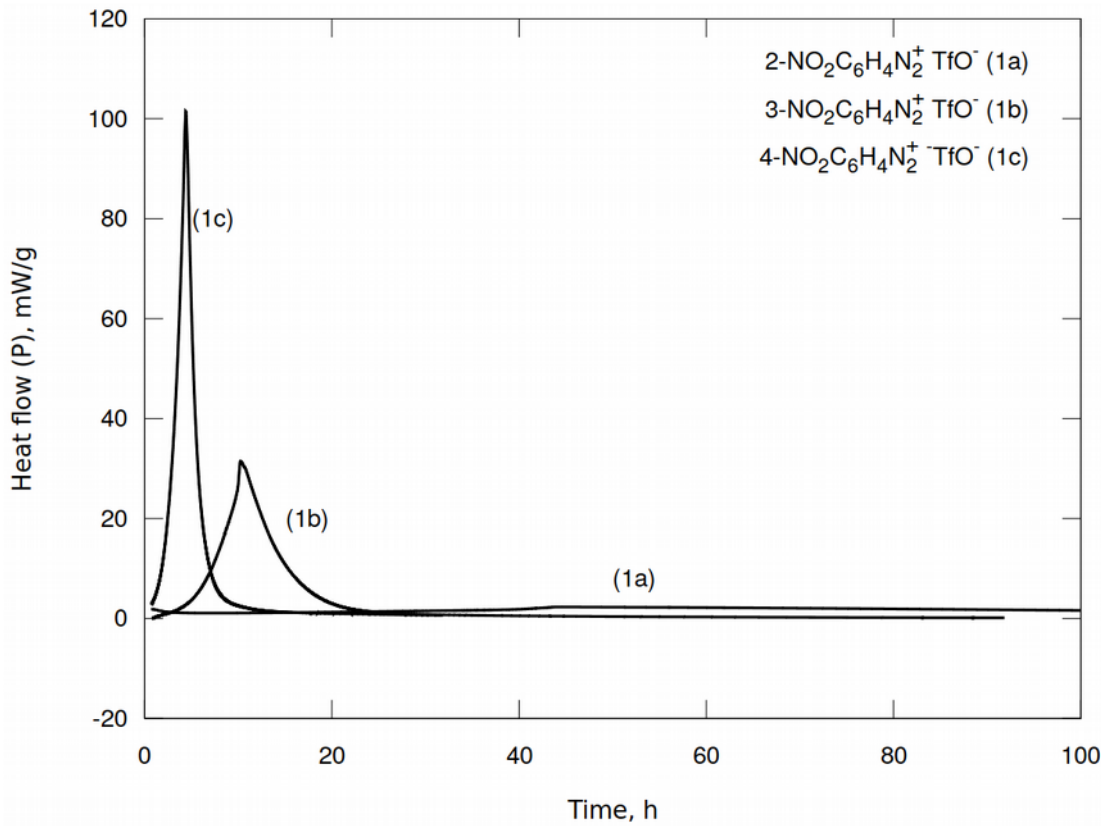


Figure 9. The heat flow (P) during isothermal decomposition of 2-, 3- and 4-nitrobenzenediazonium triflates **1a-c** at 85 °C.

The analysis of the kinetic data obtained at different temperatures followed by approximation with the Arrhenius equation allowed us to find the kinetic parameters of DS decomposition reactions occurring at 25 °C. The obtained results are presented in Table 5 and Fig. 10. The arenediazonium triflates **1b-d** have higher activation energies comparing to tosylate **2** and tetrafluoroborate **3**. However, 2-nitrobenzenediazonium triflate is out of this line as it has the lowest activation energy among the DS studied.

Table 5. The calculated kinetic parameters of DS **1-3** decomposition reactions occurring at 25 °C ( $k_{298}$  – rate constant at 298 °K; Ea — activation energy).

Diazonium salt	$k_{298}$ , g · mol <sup>-1</sup> · c <sup>-1</sup>	Ea, kJ/mol
2-NO <sub>2</sub> C <sub>6</sub> H <sub>4</sub> N <sub>2</sub> <sup>+</sup> TfO <sup>-</sup> <b>1a</b>	4.17*10 <sup>-7</sup>	111.4
3-NO <sub>2</sub> C <sub>6</sub> H <sub>4</sub> N <sub>2</sub> <sup>+</sup> TfO <sup>-</sup> <b>1b</b>	8.66*10 <sup>-7</sup>	159.7
4-NO <sub>2</sub> C <sub>6</sub> H <sub>4</sub> N <sub>2</sub> <sup>+</sup> TfO <sup>-</sup> <b>1c</b>	1.33*10 <sup>-6</sup>	173.0
4-MeOC <sub>6</sub> H <sub>4</sub> N <sub>2</sub> <sup>+</sup> TfO <sup>-</sup> <b>1d</b>	1.39*10 <sup>-8</sup>	187.1
4-NO <sub>2</sub> C <sub>6</sub> H <sub>4</sub> N <sub>2</sub> <sup>+</sup> TsO <sup>-</sup> <b>2</b>	1.39*10 <sup>-5</sup>	131.7
4-NO <sub>2</sub> C <sub>6</sub> H <sub>4</sub> N <sub>2</sub> <sup>+</sup> BF <sub>4</sub> <sup>-</sup> <b>3</b>	5.33*10 <sup>-6</sup>	140.3

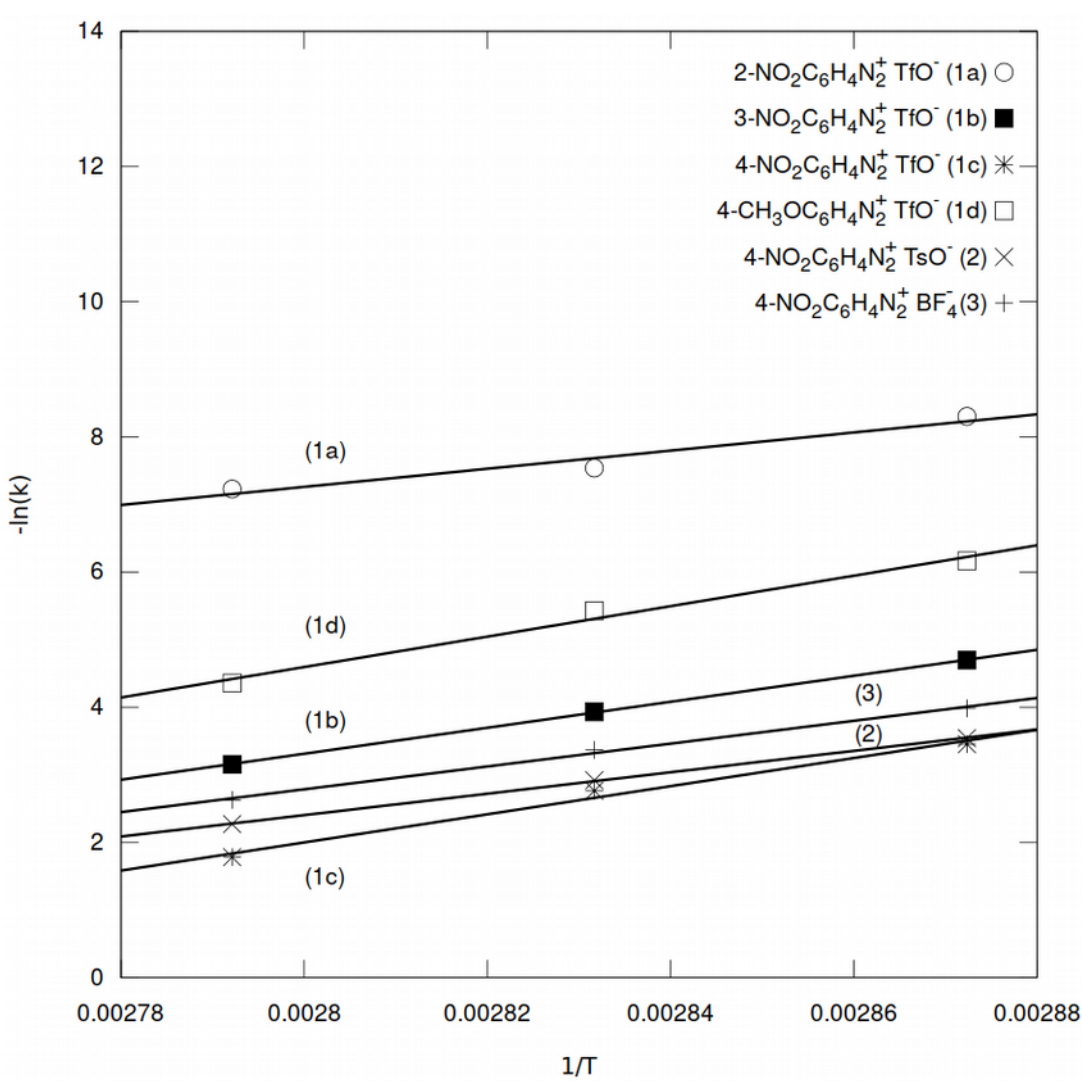


Figure 10. Results of the approximation of DS **1-3** decomposition reactions with the Arrhenius equation

Based on the approximation data, we have modeled the process of decomposition of the investigated DS over large time period (Fig. 11-12). According to the results, the stability of arenediazonium triflates depends on the substitution pattern. In particular, at 25 °C 3-

nitrobenzenediazonium triflate has the longest half-life time of 90 years, whereas 2-nitrobenzenediazonium triflate has the shortest half-life time of 25 years (Fig. 11). The nature of counterion affects greatly the DS stability (Fig. 12). Thus, 4-nitrobenzenediazonium tosylate **2** and tetrafluoroborate **3** have close half-life times of 4.5 years. Whereas 4-nitrobenzenediazonium triflate **1c** is much more stable with a half-life time of 46 years and a significantly lower maximum heat flow. Note that the effect of counterion on DS stability becomes noticeable only at low temperatures (25 °C), while at elevated temperatures (during DSC/TGA or isothermal flow calorimetry at 75–85 °C) these differences disappear. This fact, as well as the values of activation energies, suggest that the stability of DS under normal storage conditions is largely determined by the strength of the crystal lattice. At higher temperatures, after the destruction of the crystal lattice, the speed and energy of the process are likely to be influenced by both the nature of the Ar-N<sub>2</sub><sup>+</sup> diazonium cation and the presence and nature of nucleophiles in the immediate environment.

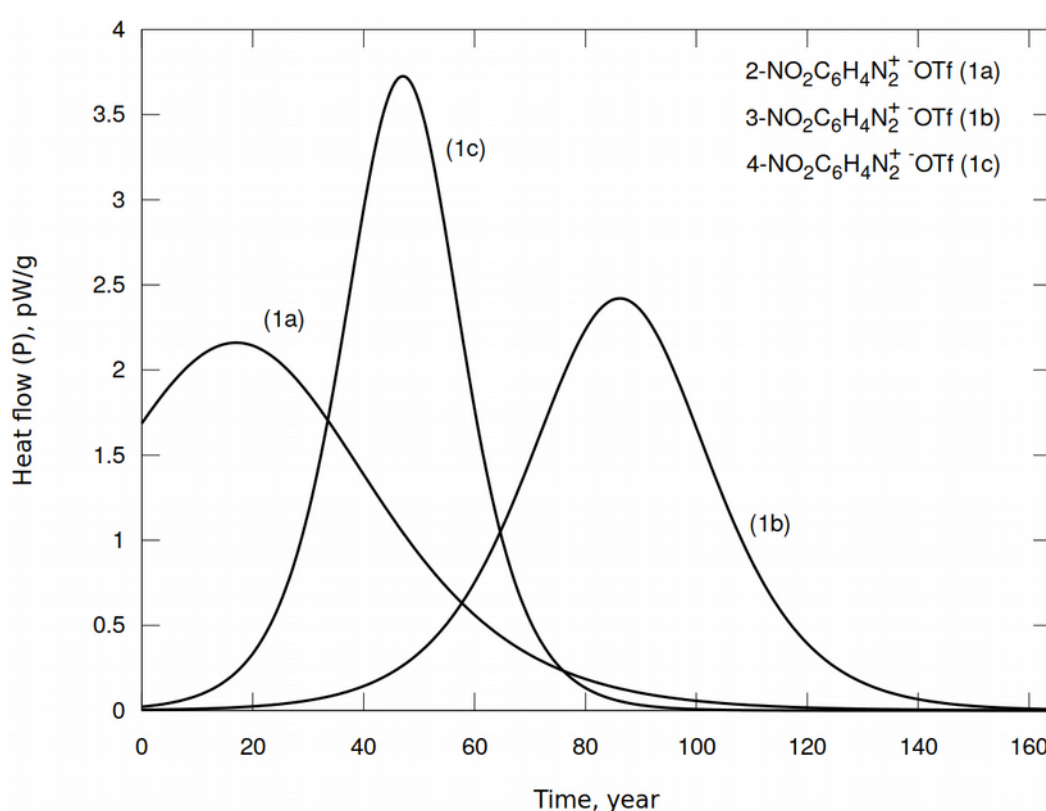


Figure 11. The heat flow (P) over the time dependency built upon modelling of the kinetic curves of the decomposition of 2-, 3- and 4-nitrobenzenediazonium triflates **1a-c** at 25 °C.

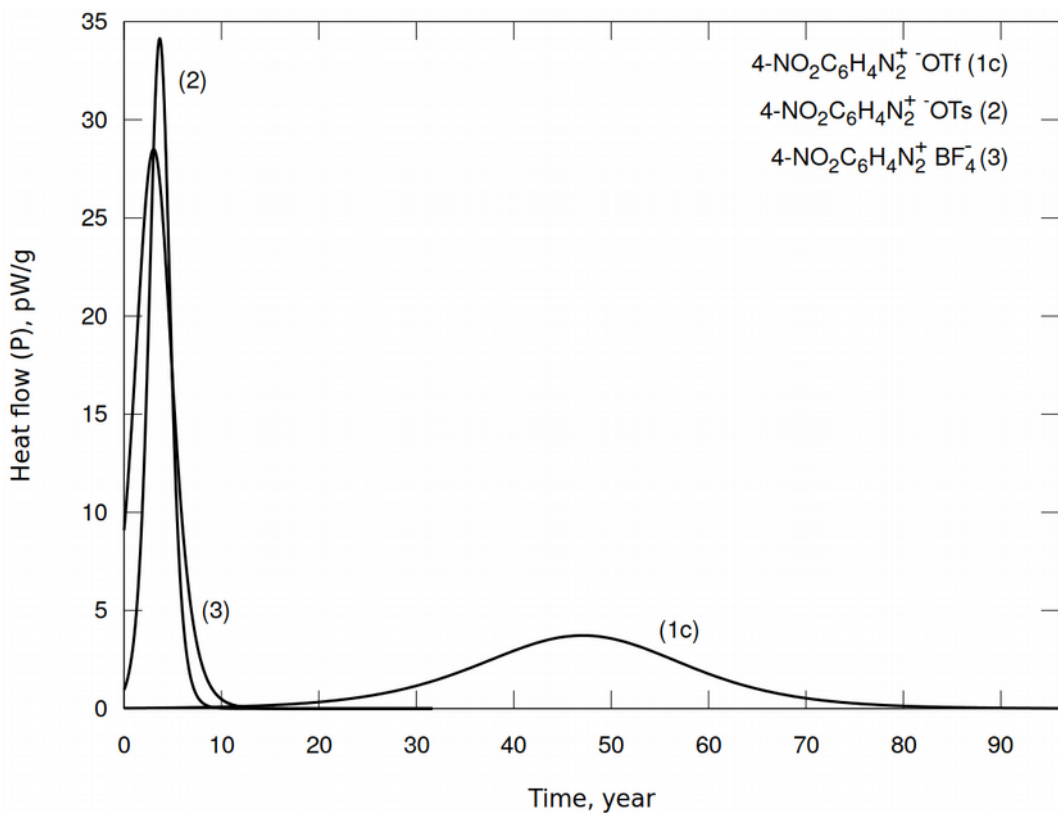


Figure 12. The heat flow (P) over the time dependency built upon modelling of the kinetic curves of the decomposition of 4-nitrobenzenediazonium tosulate **2**, triflate **1c** and tetrafluoroborate **3** at 25 °C.

Thus, considering all the data, we can draw several conclusions. First of all, DSC/TGA alone cannot serve as a reliable criterion for assessing the thermal stability and safety of DSs, since in this case decomposition occurs at higher temperatures and is accompanied by intense evaporation of low-molecular-weight reaction products. In addition, during DSC/TGA analysis DSs decompose at different temperatures, which makes the analysis and comparison of the data complicated. Therefore, the study of DS thermal stability should be complemented by a more detailed investigation of the decomposition kinetics by isothermal flow calorimetry. The values of maximum heat flow, half-lives, and activation energies should be determined and approximation of the kinetics to normal conditions should be done.

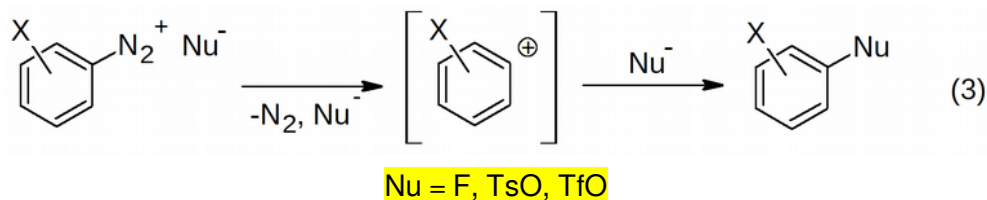
Secondly, the nature of counterion has a pronounced effect on DS stability. The approximation of experimental data with Arrhenius equation showed that arenediazonium triflates are the most stable during the storage, for example, 3-nitrobenzenediazonium triflate has a shelf-life of 90 years. Presumably, changing the counterion effects the probability of the occurrence of various mechanisms during the DS decomposition (Предположительно, влияние аниона связано с изменением вероятности протекания различных механизмов при разложении солей). {What did you mean by that?}

Finally, given the results of isothermal flow calorimetry, the DSs studied decompose with thermal effects close to the threshold value of 800 J/g for safe transportation, according to UNESCO [6]. Only in the case of 2-nitrobenzenediazonium triflate, the released energy of -1300 J/g exceeds the permissible value.

## GC-MS and LC-MS study of decomposition products

While it has long been established that the main products of the thermal decomposition of arenediazonium tetrafluoroborates are the corresponding aryl fluorides (the Balz-Schiemann reaction), the products of the thermolysis of arenediazonium triflates and tosylates remain unknown. We elucidated the structure of the compounds that appear after 14 days of decomposition of DSs **1-3** at 85 °C using GC-MS and LC-MS. To conduct the analysis, the unreacted DS was converted into corresponding aryl iodide by reaction with KI.

According to the GC-MS data (Supporting 2s, Fig. S15-20) {*I suggest assigning different numbers to figures in Supporting and add S in front of it. It is very common to do that and most of the journals would eventually force you to arrange the data in that way*}, the main products of the decomposition of DSs **1b**, **1c**, **1d** are the corresponding esters of nitro-phenyl trifluoromethanesulfonates ArOTf. The decomposition of arenediazonium tosylate **2** resulted in the formation of nitrobenzene and 1-iodo-4-nitrobenzene (GC-MS). LC-MS ESI in negative ionization mode also showed the presence of 4-nitrophenyl 4-methylbenzenesulfonate ester ( $m/z=292.1$ ) among the decomposition products. In case of arenediazonium tetrafluoroborate **3**, the main decomposition product was the expected 1-fluoro-4-nitrobenzene. It should be noted that during the decomposition of all the DSs studied, significant amounts of resinous products that could not be elucidated by GC-MS were formed. Considering the GC-MS and LC-MS results, the following mechanism can be assumed for thermolysis of DSs **1b-d**, **2**, **3** (Scheme 2).



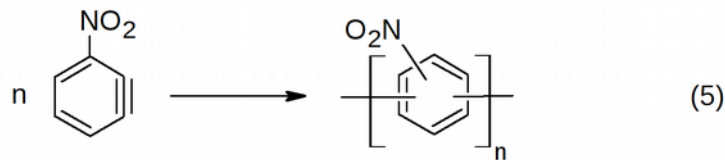
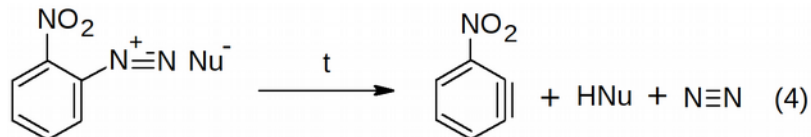
Scheme 2. The possible mechanism of thermal decomposition of DSs **1b-d**, **2**, **3** {*I would assign this as Scheme not an equation since you are providing mechanism*}

A completely different process takes place when 2-nitroarenediazonium triflate **1a** decomposes. In this case, the products of the diazonium group substitution by the triflate anion were not detected. The compounds formed during the DS **1a** decomposition were polymers. We were able to elucidate their structure by LC-MS (Table 6, MS spectra presented in Supporting 3s). The polymers found were suggested to be built upon the following repeating units:  $\text{NO}_2\text{C}_6\text{H}_3$  ( $\Delta M/Z=121.0$ ) and  $[\text{NO}_2\text{C}_6\text{H}_4\text{SCF}_3]$  ( $\Delta M/Z=223$ ).

Table 6. The main peaks present on the LC-MS chromatograms of the decomposition products of 2-nitroarenediazonium triflate **1a**

<b>Ionization Mode</b>	<b>M/Z</b>	<b>Compound</b>
Positive ESI	74.1; 297.1; 520.2; 743.2  432.1; 553.1; 674.1; 795.1; 916.1; 1037.1; 1158.1  525.1; 646.1; 767.1; 888.1; 1009.1; 1130.1  588.2; 710.1; 831.2; 952.2;  275.1; 785.8; 915.2; 1087.1	Polymer chain P1 with the mass of repeating unit of 223, possibly, $[\text{NO}_2\text{C}_6\text{H}_4\text{SCF}_3]$  Polymer chain P2 with the mass of repeating unit of 121, $[\text{C}_6\text{H}_3\text{NO}_2]$  Polymer chain P3 with the mass of repeating unit of 121, $[\text{C}_6\text{H}_3\text{NO}_2]$ <i>The difference between P2 and P3 is 28, which corresponds to the nitrogen elimination</i>  Polymer chain P4 with the mass of repeating unit of 121, $[\text{C}_6\text{H}_3\text{NO}_2]$
Positive APCI	394.0; 515.0; 635.9; 756.9; 877.8; 998.8; 1119.7  597.3; 875.4; 877.4; 879.4	Polymer chain P5 with the mass of repeating unit of 121, $[\text{C}_6\text{H}_3\text{NO}_2]$
Negative ESI	380.1; 501.1; 622.1; 743.1; 864.1  528.0; 649.1; 770.1; 891.1  149.0 276.8; 320.9; 436.7; 563.6; 936.2	Polymer chain P6 with the mass of repeating unit of 121, $[\text{C}_6\text{H}_3\text{NO}_2]$  Polymer chain P7 with the mass of repeating unit of 121, $[\text{C}_6\text{H}_3\text{NO}_2]$ $\text{TfO}^-$

Apparently, the appearance of the above-mentioned resinous compounds is associated with the polymerization processes as proven by the polymeric nature of products formed as a result of DS **1a** decomposition. We can infer that 1-nitrocyclohexa-1,3-dien-5-yne  $[\text{C}_6\text{H}_3\text{NO}_2]$  ( $\Delta M/Z=121.0$ ) is a monomer that is derived from DS according to the route presented in Scheme 3.



**Scheme 3.** Possible route of 1-nitrocyclohexa-1,3-dien-5-yne [ $C_6H_3NO_2$ ] ( $\Delta M/Z=121.0$ )  
formation (a) and further polymerization (b)

{Same is here. It may be useful to assign numbers to intermediate structures}

The mechanism of further chain growth involving  $C_6H_3NO_2$  as monomer is ambiguous and requires special investigation lying beyond the scope of this work. However, based on the available data, we can assume the structure of the polymer formed as a result of the DS **1a** decomposition (Scheme 5).

Importantly, the unique route found for DS **1a** decomposition including the formation of neutral  $C_6H_3NO_2$  is consistent with the high instability of the intermediate involved in an alternative pathway (Scheme 2). Indeed, the 2-nitrobenzene-1-ylidium cation that would be formed in this case is much less stable and energetically unfavorable comparing to cations derived from the other DSs due to fact that electron withdrawing group  $NO_2$  is next to carbocationic center.

### Quantum chemical calculations

Given the identified products of DS **1a-c**, **2**, **3** thermal decomposition, we for the first time predicted the thermodynamics of the occurring processes using DFT calculations at RB3LYP/aug-cc-pVDZ level of theory. We have optimized geometry of DS **1a-c**, **2**, **3** and diazonium group substitution products. The nature of located stationary points was confirmed by the absence of imaginary frequencies in IR spectrum. Cartesian coordinates of all compounds, and calculated thermodynamic parameters are given in Supporting 4s. We have explored esters and substituted phenols as the major products of triflates **1a-c** and tosylate **2** decomposition and 4-fluoronitrobenzene as the major product of tetrafluoroborate **3** decomposition. The predicted and experimental thermodynamic parameters of the reactions are presented in Tables 7 and 8. Considering DSC/TGA results that showed that thermolysis of tetrafluoroborate **3** initially causes  $BF_3$  cleavage with the formation of  $4-NO_2C_6H_4N_2^+F^-$  **3a** (equation 1), we calculated the thermodynamics of this reaction along with other possible routes (Table 6, entries 6a, b).

Table 7. Predicted thermodynamic parameters of DS **1a-c**, **2**, **3** decomposition reactions according to quantum chemical calculations at RB3LYP/aug-cc-pVDZ level of theory.

Entry	Reaction	$\Delta G_{298}$ ,	$\Delta H_{298}$ ,	$\Delta S^{*298.15}$ ,
-------	----------	--------------------	--------------------	------------------------

		<b>kJ/mol</b>	<b>kJ/mol</b>	<b>kJ/mol</b>
1	$2\text{-NO}_2\text{C}_6\text{H}_4\text{N}_2^+\text{-OTf} \rightarrow 2\text{-NO}_2\text{C}_6\text{H}_4\text{OTf} + \text{N}_2$	-268.6	-230.1	38.5
2	$3\text{-NO}_2\text{C}_6\text{H}_4\text{N}_2^+\text{-OTf} \rightarrow 3\text{-NO}_2\text{C}_6\text{H}_4\text{OTf} + \text{N}_2$	-282.4	-242.8	39.6
3	$4\text{-NO}_2\text{C}_6\text{H}_4\text{N}_2^+\text{-OTf} \rightarrow 4\text{-NO}_2\text{C}_6\text{H}_4\text{OTf} + \text{N}_2$	-287.6	-248.0	39.6
4	$4\text{-MeOC}_6\text{H}_4\text{N}_2^+\text{-OTf} \rightarrow 4\text{-MeOC}_6\text{H}_4\text{OTf} + \text{N}_2$	-238.1	-200.5	37.7
5	$4\text{-NO}_2\text{C}_6\text{H}_4\text{N}_2^+\text{-OTs} \rightarrow 4\text{-NO}_2\text{C}_6\text{H}_4\text{OTs} + \text{N}_2$	-328.4	-283.9	44.6
6	$4\text{-NO}_2\text{C}_6\text{H}_4\text{N}_2^+\text{-BF}_4 \rightarrow 4\text{-NO}_2\text{C}_6\text{H}_4\text{F} + \text{BF}_3 + \text{N}_2$	-276.2	-188.4	87.9
6a	$4\text{-NO}_2\text{C}_6\text{H}_4\text{N}_2^+\text{-BF}_4 \rightarrow 4\text{-NO}_2\text{C}_6\text{H}_4\text{N}_2\text{F} + \text{BF}_3$	76.2	124.6	48.5
6b	$4\text{-NO}_2\text{C}_6\text{H}_4\text{N}_2\text{F} \rightarrow 4\text{-NO}_2\text{C}_6\text{H}_4\text{F} + \text{N}_2$	-352.3	-312.9	39.4

Table 8. Experimental and predicted enthalpies of decomposition of diazonium salts (RB3LYP/aug-cc-pVDZ).

<b>Reaction</b>	<b>Predicted enthalpy</b>	<b>Experimental enthalpy (flow calorimetry)</b>			<b>DSC/TGA</b>
	$\Delta H_{298}, (\Delta H_{353})$ <b>kJ/mol</b>	$\Delta H_{348}$ , <b>kJ/mol</b>	$\Delta H_{353}$ , <b>kJ/mol</b>	$\Delta H_{358}$ , <b>kJ/mol</b>	
$2\text{-NO}_2\text{C}_6\text{H}_4\text{N}_2^+\text{-OTf} \rightarrow 2\text{-NO}_2\text{C}_6\text{H}_4\text{OTf} + \text{N}_2$	-230 (-230.4)	-414	-386	-396	-203.4
$3\text{-NO}_2\text{C}_6\text{H}_4\text{N}_2^+\text{-OTf} \rightarrow 3\text{-NO}_2\text{C}_6\text{H}_4\text{OTf} + \text{N}_2$	-243 (-243.2)	-228	-230	-225	-238.5
$4\text{-NO}_2\text{C}_6\text{H}_4\text{N}_2^+\text{-OTf} \rightarrow 4\text{-NO}_2\text{C}_6\text{H}_4\text{OTf} + \text{N}_2$	-248 (-248.4)	-200	-235	-250	-65.8
$4\text{-MeOC}_6\text{H}_4\text{N}_2^+\text{-OTf} \rightarrow 4\text{-MeOC}_6\text{H}_4\text{OTf} + \text{N}_2$	-201 (-200.8)	-183	-183	-106	-64.5
$4\text{-NO}_2\text{C}_6\text{H}_4\text{N}_2^+\text{-OTs} \rightarrow 4\text{-NO}_2\text{C}_6\text{H}_4\text{OTs} + \text{N}_2$	-284 (-284.0)	-253	-232	-231	-117.3
$4\text{-NO}_2\text{C}_6\text{H}_4\text{N}_2^+\text{-BF}_4 \rightarrow 4\text{-NO}_2\text{C}_6\text{H}_4\text{F} + \text{BF}_3 + \text{N}_2$	-188 (-189.5)	-173	-156	-147	-54.3

Overall, for all reactions of DS **1b-d**, **2** and **3** decomposition the calculated enthalpy values are consistent with the experimental ones obtained by isothermal flow calorimetry. Therefore, the suggested reactions make the main contribution to the energy of DS exothermic decomposition (Table 6, 7). The obtained results prove that DFT calculations at RB3LYP/aug-cc-pVDZ level of theory is a convenient and fairly precise method for theoretical estimation of the thermal effects of DS decomposition. A single case where we had significant deviation between the data of isothermal flow calorimetry and calculation results is 2-nitroarenediazonium triflate **1a** (Table 7). However, this is consistent with GC-MS and LC-MS data demonstrating that decomposition of DS **1a** proceeds via different route (**Scheme 4 and 5**) and does not result in  $2\text{-NO}_2\text{C}_6\text{H}_4\text{OTf}$ .

In some cases, the enthalpy values of DS **1-3** exothermic decomposition measured by DSC/TGA were found to be significantly less than both predicted ones and values obtained by isothermal flow calorimetry (Table 8). It can be explained by the fact that decomposition of DSs during DSC/TGA analysis occurs at temperatures much higher than  $85^\circ\text{C}$  (Table 2), resulting in an evaporation process, accompanied by a significant weight loss, which reduces the thermal effect of the reaction.

## CONCLUSIONS

In conclusion, for the first time we have determined the thermodynamics and kinetics of thermal decomposition of a series of aromatic diazonium salts  $\text{ArN}_2^+\text{X}^-$  with various counterions X = TfO, TsO, BF<sub>4</sub> by isothermal flow calorimetry and provided the quantitative assessment of the storage stability of solid DSs under normal conditions. Additionally, we have established how the aromatic substitution pattern in diazonium cation and the nature of counterion effect the processes occurring during the thermolysis of DSs studied.

We demonstrated that thermodynamic parameters of DS thermal decomposition reactions calculated by DFT at RB3LYP/aug-cc-pVDZ are consisted with experimental data obtained by isothermal flow calorimetry for all 3- and 4-substituted DSs investigated (**1b-d, 2, 3**). For these DSs the main decomposition route is elimination of nitrogen with the formation of benzene-1-ylum ions that subsequently react with the corresponding anions. A completely different process occurs during the thermolysis of 2-nitrobenzene diazonium triflate **1a**. In this case, the polymeric products are formed, probably through the primary generation of 1-nitrocyclohexa-1,3-dien-5-yne.

## ASSOCIATED CONTENT

### AUTHOR INFORMATION

### ACKNOWLEDGMENTS

### REFERENCES (FINAL)

- (1) (a) Zollinger, H. *Diazo Chemistry I: Aromatic and Heteroaromatic Compounds*; VCH, Weinheim, **1994**. (b) Roglands, A.; Pla-Quintana, A.; Moreno-Manas M. *Chem. Rev.* **2006**, *106*, 4622. (c) Bonin H.; Fouquet, E.; Felpin, F.-X. *Adv. Synth. Catal.* **2011**, *353*, 3063. (d) Mo, F.; Dong, G.; Zhang, Y.; Wang, J. *Org. Biomol. Chem.* **2013**, *11*, 1582. (e) Kölmel, D. K.; Jung, N.; Bräse, S. *Aust. J. Chem.* **2014**, *67*, 328. (f) Deadman, B. J.; Collins, S.G.; Maguire, A. R. *Chem.Eur. J.* **2015**, *21*, 2298. (g) Idowu, O.S., Kolawole, A.O., Abegoke, O.A., Kolade, Y.T., Fasanmade, A.A., Olaniyi, A.A. *J. AOAC International*, **2005**, *88*, 1108.
- (2) Mahouche-Chergui, S.; Gam-Derouich, S.; Manganey, C.; Chehimi, M. M. *Chem. Soc. Rev.* **2011**, *40*, 4143.
- (3) (a) Filimonov V. D., Trusova M.E., Postnikov P.S., Krasnokutskaya E.A., Lee Y.M., Hwang H.Y., Kim H., Ki-Whan Chi. Unusually Stable, Versatile, and Pure Arenediazonium Tosylates: their Preparation, Structures, and Synthetic Applicability. *Org. Lett.*, **2008**, *10*, 3961-3964. (b) V.D. Filimonov, E.A. Krasnokutskaya, A.Zh. Kassanova, V.A. Fedorova, K.S. Stankevich, N.G. Naumov, A.A. Bondarev, V.A. Kataeva. Synthesis, structure, and synthetic potential of arenediazonium trifluoromethanesulfonates as stable and safe diazonium salts. *Eur. J. Org. Chem.* **2018**, <https://doi.org/10.1002/ejoc.201800887>
- (4) (a) Krasnokutskaya E.A., Semenischeva N.I., Filimonov V.D., Knochel P. *Synthesis*, 2007, 81. (b) Filimonov V.D., Semenischeva N.I., Krasnokutskaya E.A., Tretyakov A.N., Hwang H.Y., Chi K.-W. Sulfonic Acid Based Cation-Exchange Resin: A Novel Proton Source for One-Pot Diazotization-

Iodination of Aromatic Amines in Water. *Synthesis*, **2008**, 185-187. (c) Gorlushko D.A., Filimonov V.D., Krasnokutskaya E.A., Semenischeva N.I., Go B.S., Hwang H.Y., Chi K-W. Iodination of aryl amines in a water-paste form via stable aryl diazonium tosylates. *Tetrahedron Lett.*, **2008**, 49, 1080-1082. (d) Lee Y.M., Moon M.E., Vajpayee V., Filimonov V.D., Chi K.-W. Efficient and economic halogenation of aryl amines via arenediazonium tosylate salts. *Tetrahedron*, **2010**, 66, 7418-7422. (e) Moon M.E., Choi Y., Lee Y.M., Vajpayee V., Trusova M.E., Filimonov V.D., Chi K.-W.. An expeditious and environmentally benign preparation of aryl halides from aryl amines by solvent-free grinding. *Tetrahedron Lett.*, **2010**, 51, 6769–6771. (f) Trusova M.E., Krasnokutskaya E.A. Postnikov, P.S., Choi Y.; Chi, Ki-Whan, Filimonov V.D., A Green Procedure for the Diazotization-Iodination of Aromatic Amines under Aqueous, Strong-Acid-Free Conditions. *Synthesis*, **2011**, 2154-2158. (g) Kutanova, K.V.; Trusova, M.E.; Postnikov, P.S.; Filimonov, V.D.; Parelo, J. A Simple and Effective Synthesis of Aryl Azides via Arenediazonium Tosylates. *Synthesis*. **2013**, 45, 2706-2710. (h) Kutanova, K. S.; Trusova, M. E.; Stankevich, A. V.; Postnikov, P. S.; Filimonov, V. D. Matsuda-Heck reaction with arenediazonium tosylates in water. *Beilstein J. Org. Chem.* **2015**, 11, 358-362. (i) Kutanova K.V., Jung N., Trusova M.E., Filimonov V.D., Postnikov P.S., Brase S. Arenediazonium Tosylates (ADTs) as Efficient Reagents for Suzuki-Miyaura Cross-Coupling in Neat Water. *Synthesis* **2017**, 49, 1680-1688. (j) Vajpayee, V.; Song, Y. H.; Ahn, J. S.; Chi, K.-W. *Bull. Korean Chem. Soc.* **2011**, 32, 2970.

(5) (a) Riss, P. J.; Kuschel, S.; Aigbirhio, F. I. [title](#) *Tetrahedron Lett.* 2012, 53, 1717. (b) Velikorodov, A. V.; Ionova, V. A.; Temirbulatova, S. I.; Suvorova, M. A. [title](#) *Rus. J. Org. Chem.* 2013, 49, 1004. (c) Tang, Z. Y.; Zhang, Y.; Wang, T.; Wang, W. [title](#) *Synlett.* 2010, 804. (d) PostnikovP.S., M. E. Trusova, T. A. Fedushchak, M. A. Uimin, A. E. Ermakov, V. D. Filimonov Aryldiazonium Tosylates as New Efficient Agents for Covalent Grafting of Aromatic Groups on Carbon Coatings of Metal Nanoparticles. *Nanotechnologies in Russia.* 2010, 5, 446-449 (e) Min, M.; Seo, S.; Lee, J.; Lee, S. M.; Hwang, E.; Lee, H. *Chem. Commun.* [title](#) 2013, 49, 6289.

(6) <http://www.unece.org/trans/danger/danger.html>

(7) (a) R. Ullrich, Th. Grewer, Decomposition of aromatic diazonium compounds, *Thermochim. Acta*, 1993, 225, 201-211, (b) L.L. Brown, J.S. Drury, Nitrogen Isotope Effects in the Decomposition of Diazonium Salts, *J. Chem. Phys.* 1965, 43, [1688-1691](#). (c) P.D. Storey, Calorimetric Studies of the Thermal Explosion Properties of Aromatic Diazonium Salts, *Institution. Chem. Eng. Symposium Series* 1981, [No. 68. P. 1-3. P. 9](#)

(8) P. Guillaume, M. Rat, S. Wilker, G. Pantel, Microcalorimetric and Chemical Studies of Propellants Proc. Int Annu. Conf. ICT 29, 133 (1998).

(9) (a) Williams, T. and Kelley, C. (2011). Gnuplot 4.5: an interactive plotting program. URL <http://gnuplot.info>. (Last accessed: 2011 June 7) (b) R Core Team (2017). R: A language and environment for statistical computing. R Foundation for Statistical / Computing, Vienna, Austria. URL <https://www.R-project.org/>

(10) (a) Sturm et al., BMC Bioinformatics (2008), 9, 163, (b) Kohlbacher et al., Bioinformatics (2008), 23:e191-e197

(11) Gaussian 09, Revision A.02, M. J. Frisch, G. W. Trucks, H. B. Schlegel, G. E. Scuseria, M. A. Robb, J. R. Cheeseman, G. Scalmani, V. Barone, G. A. Petersson, H. Nakatsuji, X. Li, M. Caricato, A. Marenich, J. Bloino, B. G. Janesko, R. Gomperts, B. Mennucci, H. P. Hratchian, J. V. Ortiz, A. F. Izmaylov, J. L. Sonnenberg, D. Williams-Young, F. Ding, F. Lipparini, F. Egidi, J. Goings, B. Peng, A. Petrone, T. Henderson, D. Ranasinghe, V. G. Zakrzewski, J. Gao, N. Rega, G. Zheng, W. Liang, M. Hada, M. Ehara, K. Toyota, R. Fukuda, J. Hasegawa, M. Ishida, T. Nakajima, Y. Honda, O. Kitao, H. Nakai, T. Vreven, K. Throssell, J. A. Montgomery, Jr., J. E. Peralta, F. Ogliaro, M. Bearpark, J. J. Heyd, E. Brothers, K. N. Kudin, V. N. Staroverov, T. Keith, R. Kobayashi, J. Normand, K. Raghavachari, A. Rendell, J. C. Burant, S. S. Iyengar, J. Tomasi, M. Cossi, J. M. Millam, M. Klene, C. Adamo, R. Cammi, J. W. Ochterski, R. L. Martin, K. Morokuma, O. Farkas, J. B. Foresman, and D. J. Fox, Gaussian, Inc., Wallingford CT, 2016.

## SUPPORTING

### Supporting 1s. Results of modeling and deconvolution of heat flow experimental kinetic curves acquired in isothermal conditions

The initial experimental heat flow over time curves are can be found in Supporting/Flow-Calorimetry/Main-Experiment/Source. The results of simulations when a single autocatalytic process was taken as model are presented in Supporting/Flow-Calorimetry/Main-Experiment/pdf. The results of statistical processing and assessment of data reproducibility can be found in Supporting/Flow-Calorimetry/Stat.

Deconvolution was performed by computer simulation of combinations of two independent and two consecutive autocatalytic reactions with varying values of thermal effects and kinetic parameters and minimization of the standard deviation from the experimental curve using the Broyden–Fletcher–Goldfarb–Shanno algorithm (BFGS) [1a] implemented in our computer program [1b], as well as Nelder–Mead [1c] method implemented in the R statistics software package for statistical analysis and processing [2]. The initial values for the first approximation were taken from the DSC-TGA data (endothermic reaction). Figure 1s.1-6 shows the results of deconvolution. The model of two independent autocatalytic processes was found to describe the experimental dependencies more accurately.

Table 1s.1. The result of the deconvolution of the heat flow measured during the isothermal decomposition of 2-nitrobenzenediazonium triflate **1a** using the model of two independent autocatalytic processes.

T °C	k <sub>1</sub>	k <sub>2</sub>	C <sub>01</sub>	C <sub>02</sub>	dH <sub>1</sub>	dH <sub>2</sub>	Quality
75	0.5222	0.0480	0.00133	0.00304	48.5	-500.6	7.3·10 <sup>-10</sup>
80	0.4046	0.0489	0.00111	0.00230	30.7	-441.0	7.1·10 <sup>-9</sup>
85	0.9554	0.0611	0.00070	0.00272	32.5	-453.9	1.3·10 <sup>-8</sup>

Table 1s.2. The result of the deconvolution of the heat flow measured during the isothermal decomposition of 2-nitrobenzenediazonium triflate **1a** using the model of two consecutive autocatalytic processes.

T °C	k <sub>1</sub>	k <sub>2</sub>	C <sub>01</sub>	C <sub>02</sub>	dH <sub>1</sub>	dH <sub>2</sub>	Quality
75	0.4679	0.0642	0.00191	0.00204	39.2	-520.7	1.1·10 <sup>-9</sup>
80	0.5791	0.0435	0.00122	0.00263	36.7	-493.9	6.1·10 <sup>-9</sup>
85	1.0512	0.0631	0.00075	0.00259	31.8	-483.4	1.3·10 <sup>-8</sup>

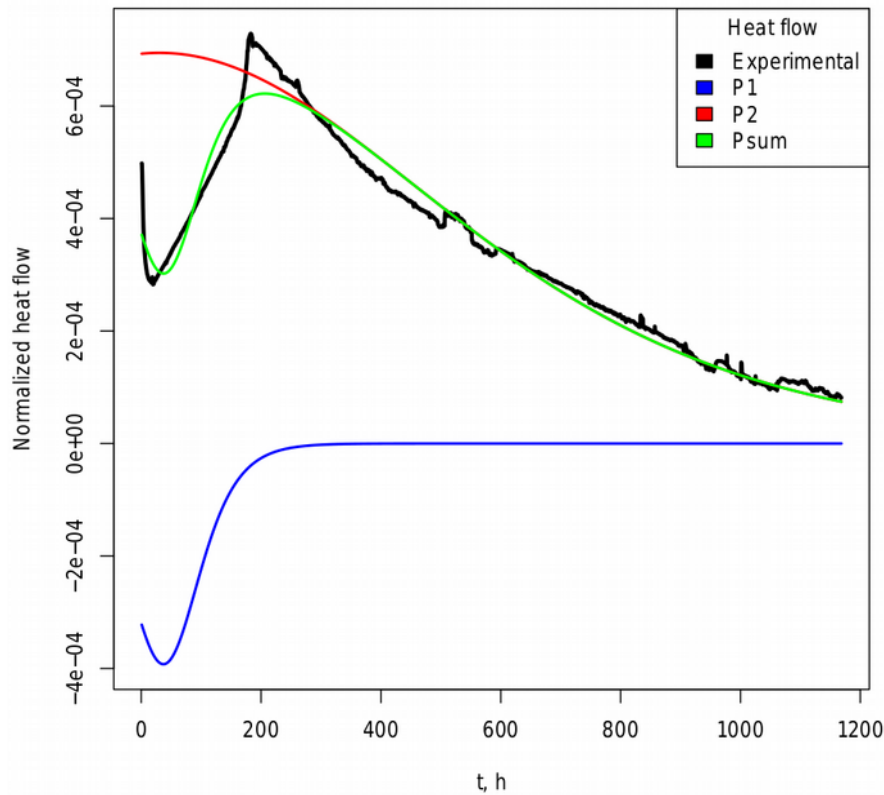


Figure 1s.1. The heat flow experimental curve and its deconvolution results for the isothermal decomposition of 2-nitrobenzenediazonium triflate **1a** at 75 °C. The deconvolution was done using the model of two independent autocatalytic processes.

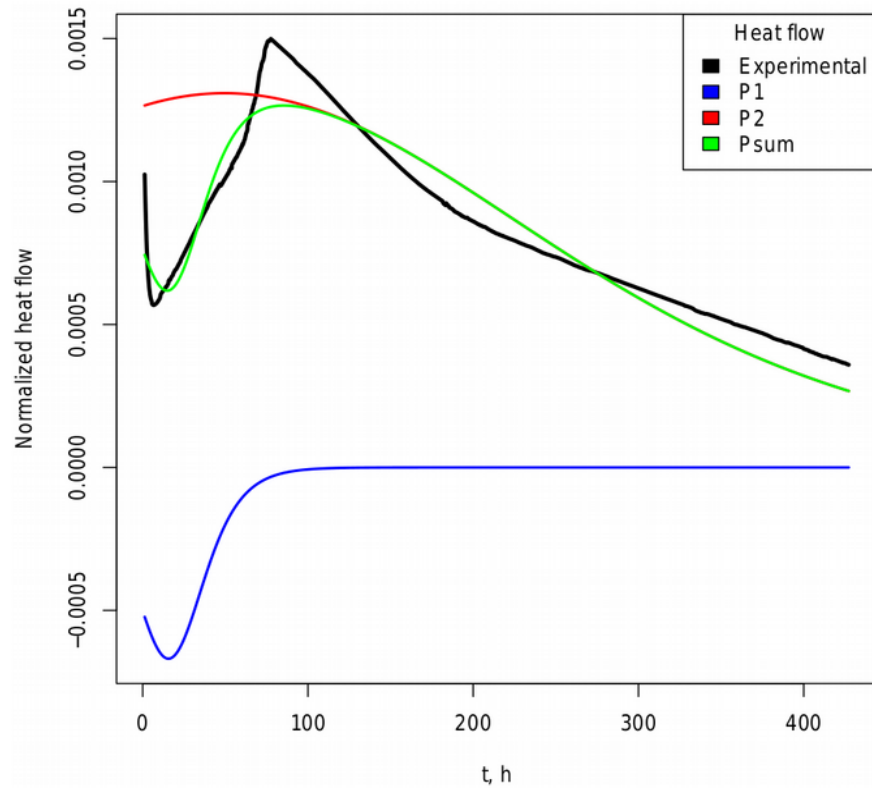


Figure 1s.2. The heat flow experimental curve and its deconvolution results for the isothermal decomposition of 2-nitrobenzenediazonium triflate **1a** at 80 °C. The deconvolution was done using the model of two independent autocatalytic processes.

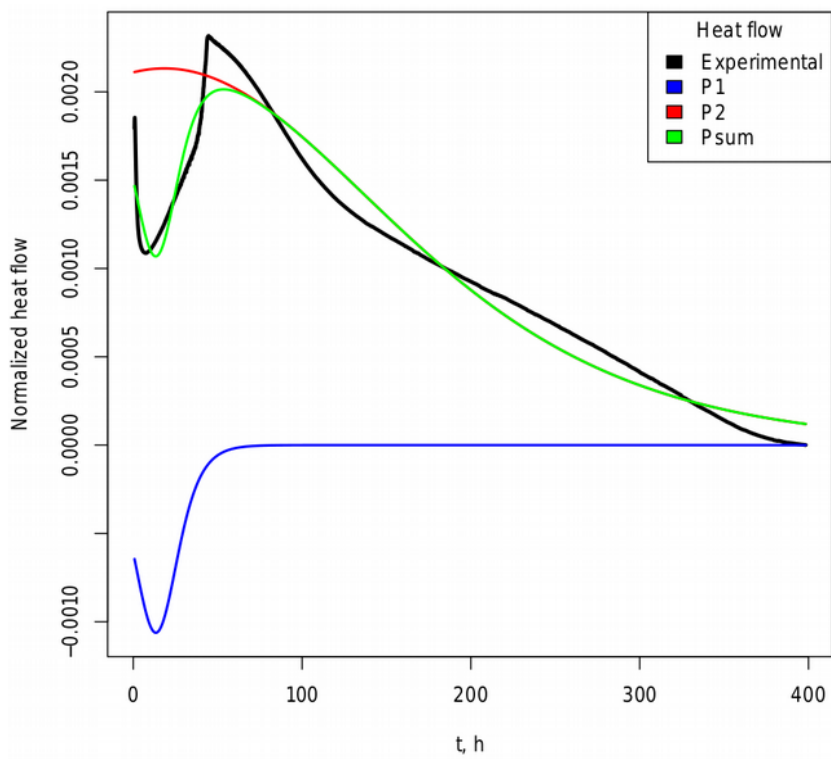


Figure 1s.3. The heat flow experimental curve and its deconvolution results for the isothermal decomposition of 2-nitrobenzenediazonium triflate **1a** at 85 °C. The deconvolution was done using the model of two independent autocatalytic processes.

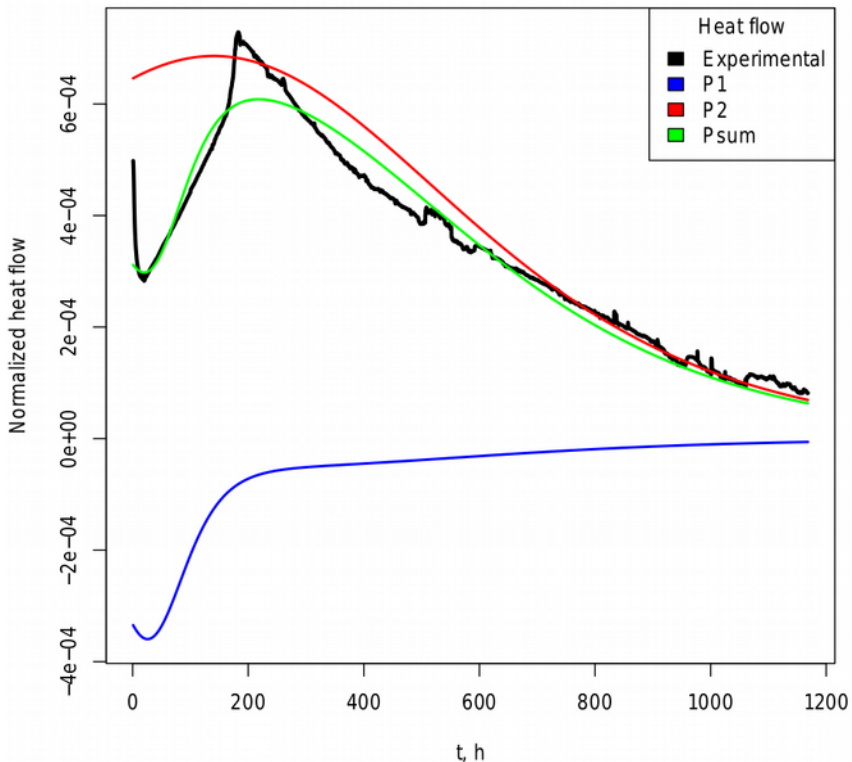


Figure 1s.4. The heat flow experimental curve and its deconvolution results for the isothermal decomposition of 2-nitrobenzenediazonium triflate **1a** at 75 °C. The deconvolution was done using the model of two consecutive autocatalytic processes.

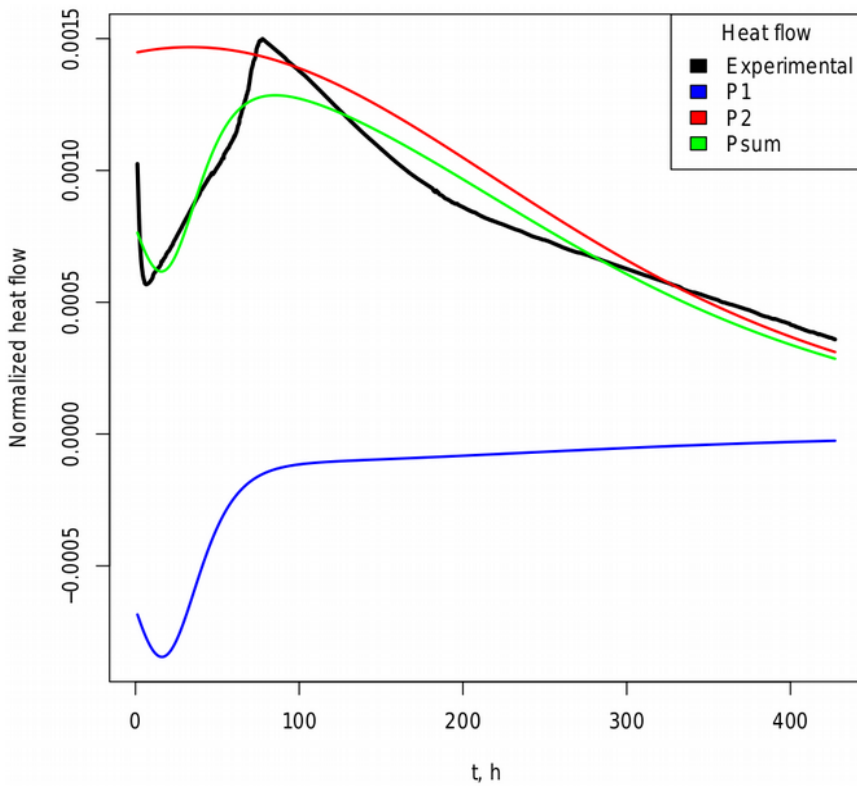


Figure 1s.5. The heat flow experimental curve and its deconvolution results for the isothermal decomposition of 2-nitrobenzenediazonium triflate **1a** at 80 °C. The deconvolution was done using the model of two consecutive autocatalytic processes.

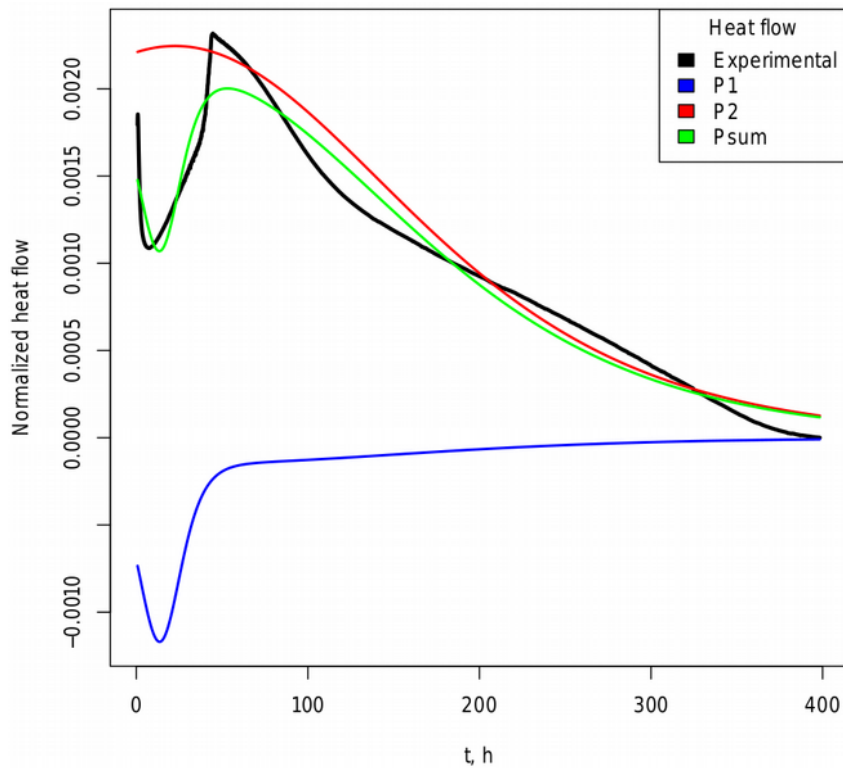


Figure 1s.6. The heat flow experimental curve and its deconvolution results for the isothermal decomposition of 2-nitrobenzenediazonium triflate **1a** at 85 °C. The deconvolution was done using the model of two consecutive autocatalytic processes.

## REFERENCES

- (1) (a) Fletcher, Roger (1987), Practical methods of optimization (2nd ed.), New York: John Wiley & Sons, ISBN 978-0-471-91547-8, (b) Alexander Bondarev. Deconvolution-Kinetic. Zenodo November 7, 2018, p. DOI: 10.5281/zenodo.1478946, (c) J.A. Nelder and R. Mead, Computer Journal, 1965, vol 7, pp 308—313, doi:10.1093/comjnl/7.4.308
- (2) (9) (a) Williams, T. and Kelley, C. (2011). Gnuplot 4.5: an interactive plotting program. URL <http://gnuplot.info>. (Last accessed: 2011 June 7) (b) R Core Team (2017). R: A language and environment for statistical computing. R Foundation for Statistical / Computing, Vienna, Austria. URL <https://www.R-project.org/>

## Supporting 2s. GC-MS spectra of the decomposition products of diazonium salts studied

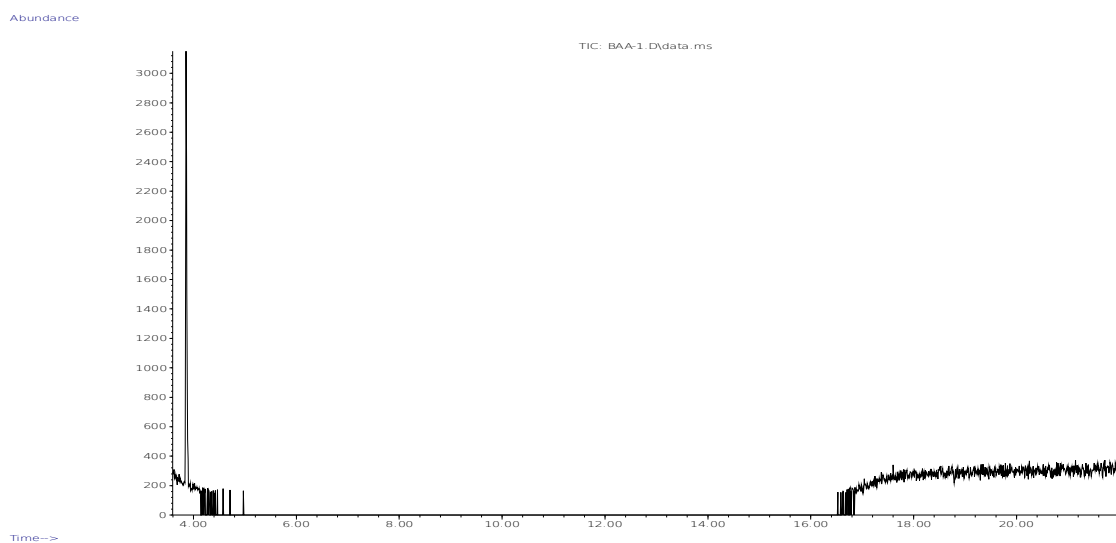


Figure 15. The decomposition products of DS **1a** according to GC-MS data.

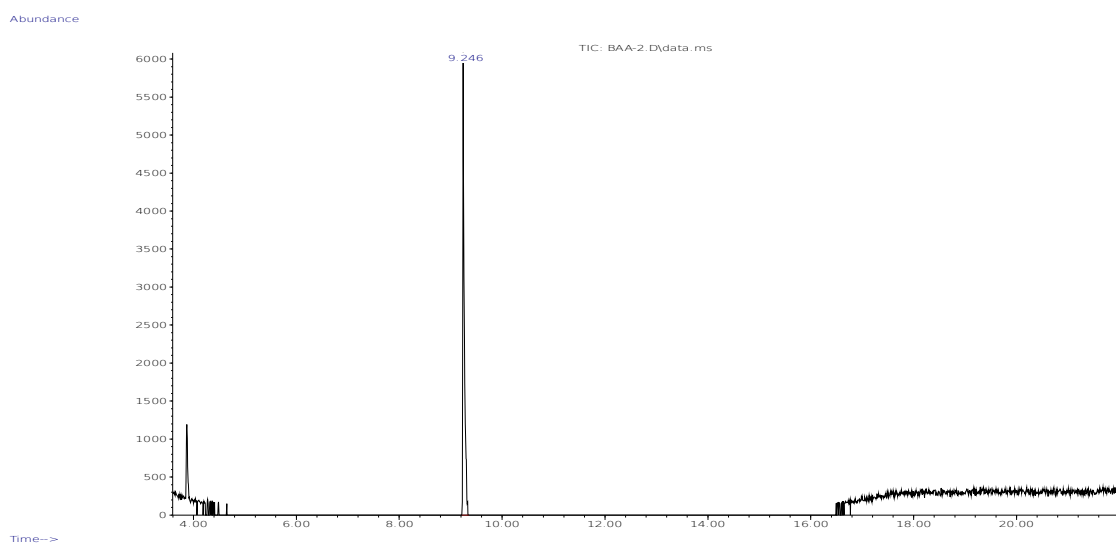


Figure 16. The decomposition products of DS **1b** according to GC-MS data. (Peak at 9.246 min corresponds to compound 3-NO<sub>2</sub>-C<sub>6</sub>H<sub>4</sub>-OSO<sub>2</sub>CF<sub>3</sub>, Fig. 21)

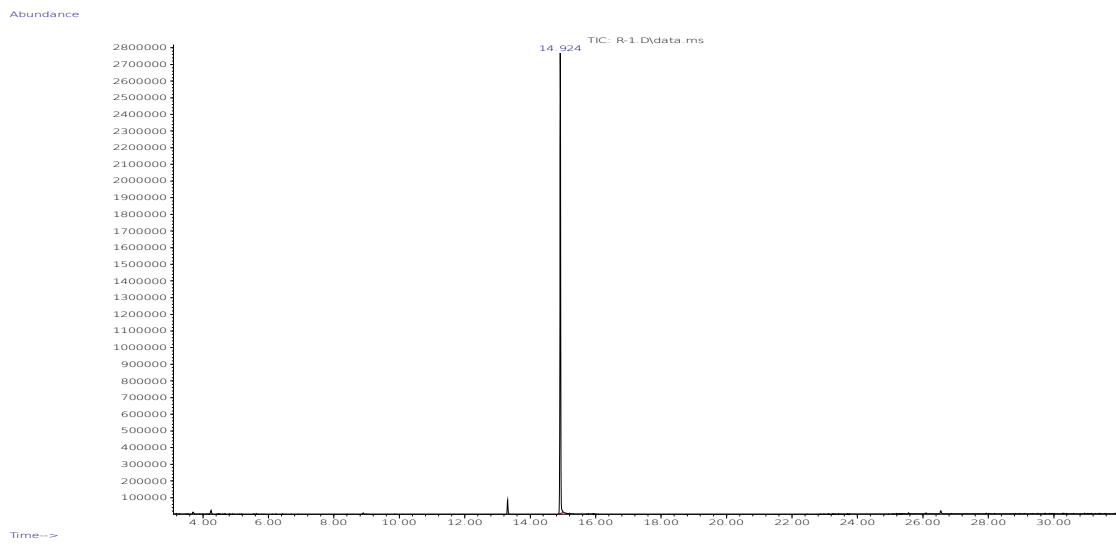


Figure 17. The decomposition products of DS **1c** according to GC-MS data. (Peak at 13.314 min corresponds to compound 4-NO<sub>2</sub>-C<sub>6</sub>H<sub>4</sub>-OSO<sub>2</sub>CF<sub>3</sub>, peak at 14.912 min corresponds to compound 1-iodo-4-nitrobenzene, Fig. 22)

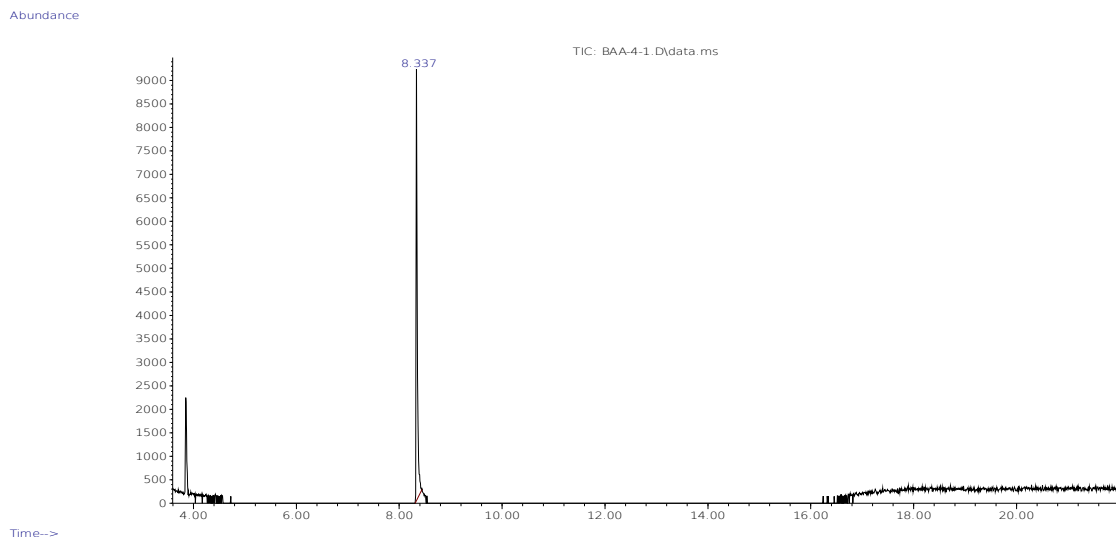


Figure 18. The decomposition products of DS **1d** according to GC-MS data. (Peak at 8.337 min corresponds to compound 4-CH<sub>3</sub>O-C<sub>6</sub>H<sub>4</sub>-OSO<sub>2</sub>CF<sub>3</sub>, Fig. 23)

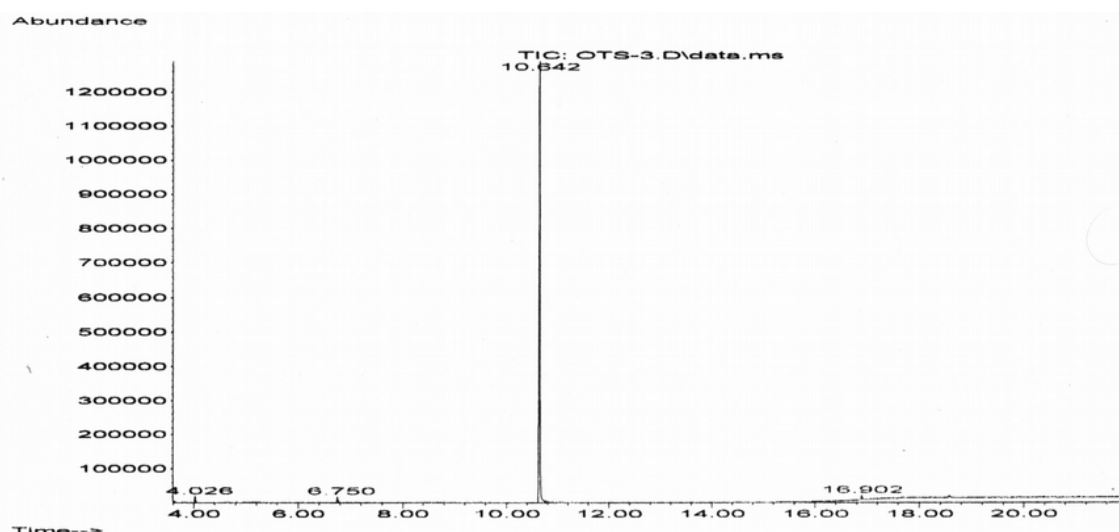


Figure 19. The decomposition products of DS **2** according to GC-MS data. (Peak at 6.750 min corresponds to 1-fluoro-4-nitrobenzene, peak at 10.642 min corresponds to 1-iodo-4-nitrobenzene,  
Fig. 24)

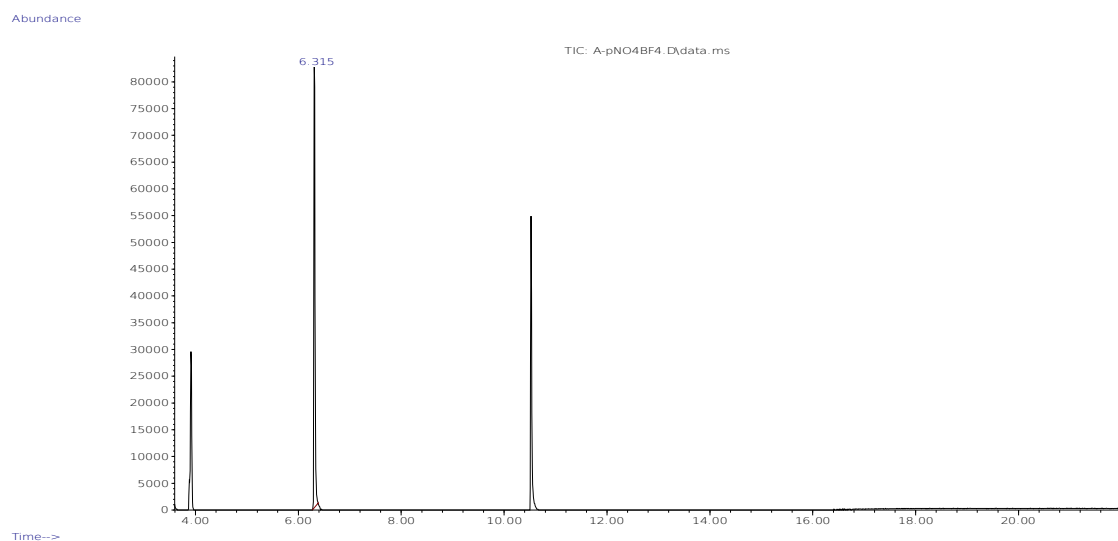


Figure 20. The decomposition products of DS **3** according to GC-MS data. (Peak at 6.307 min corresponds to 1-fluoro-4-nitrobenzene, peak at 10.515 min corresponds to 1-iodo-4-nitrobenzene,  
Fig. 25)

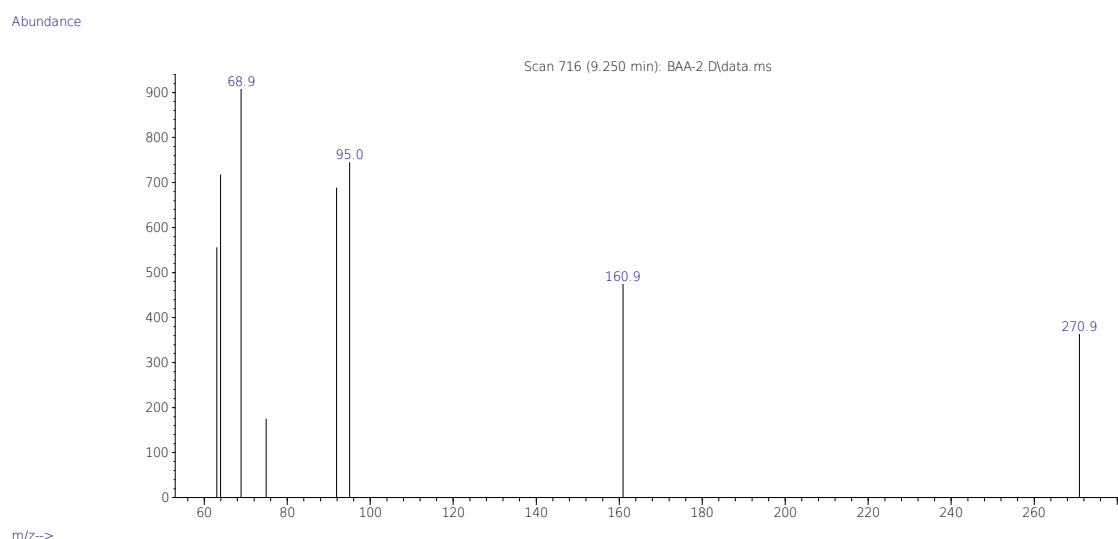


Figure 21. The major product of decomposition of DS **1b** according to GC-MS data. Fragmentation pattern corresponds to 3-NO<sub>2</sub>-C<sub>6</sub>H<sub>4</sub>-OSO<sub>2</sub>CF<sub>3</sub> M/Z: 271, 161, 95, 92, 69, 64.

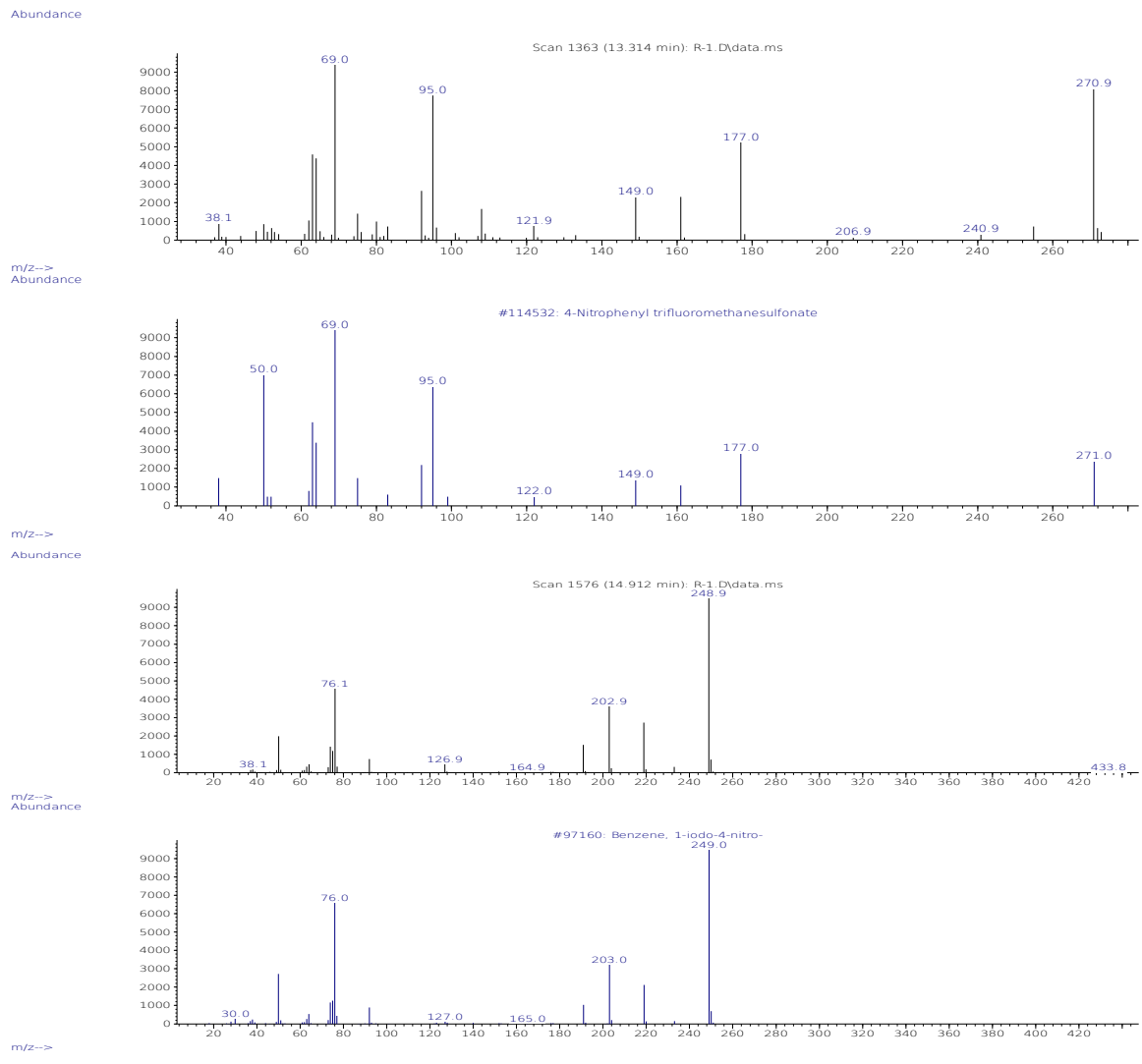


Figure 22. The major products of decomposition of DS **1c** according to GC-MS data. Fragmentation patterns correspond to  $4\text{-NO}_2\text{-C}_6\text{H}_4\text{-OSO}_2\text{CF}_3$  M/Z: 271, 177, 95, 69 and 1-iodo-4-nitrobenzene M/Z: 249, 203, 76.

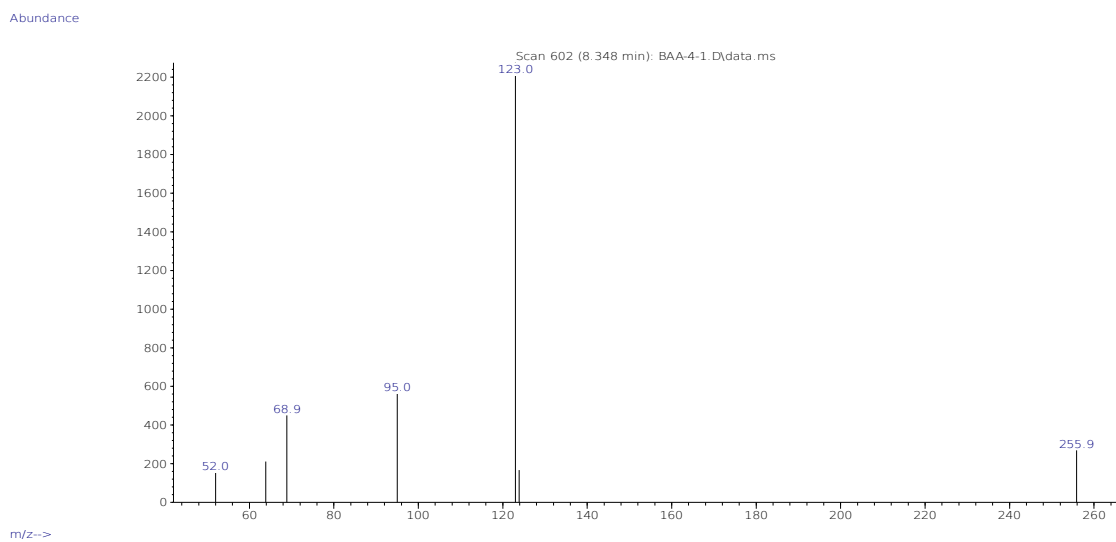


Figure 23. The major product of decomposition of DS **1d** according to GC-MS data. Fragmentation pattern corresponds to  $3\text{-CH}_3\text{O-C}_6\text{H}_4\text{-OSO}_2\text{CF}_3$  M/Z: 256, 123, 69, 52.

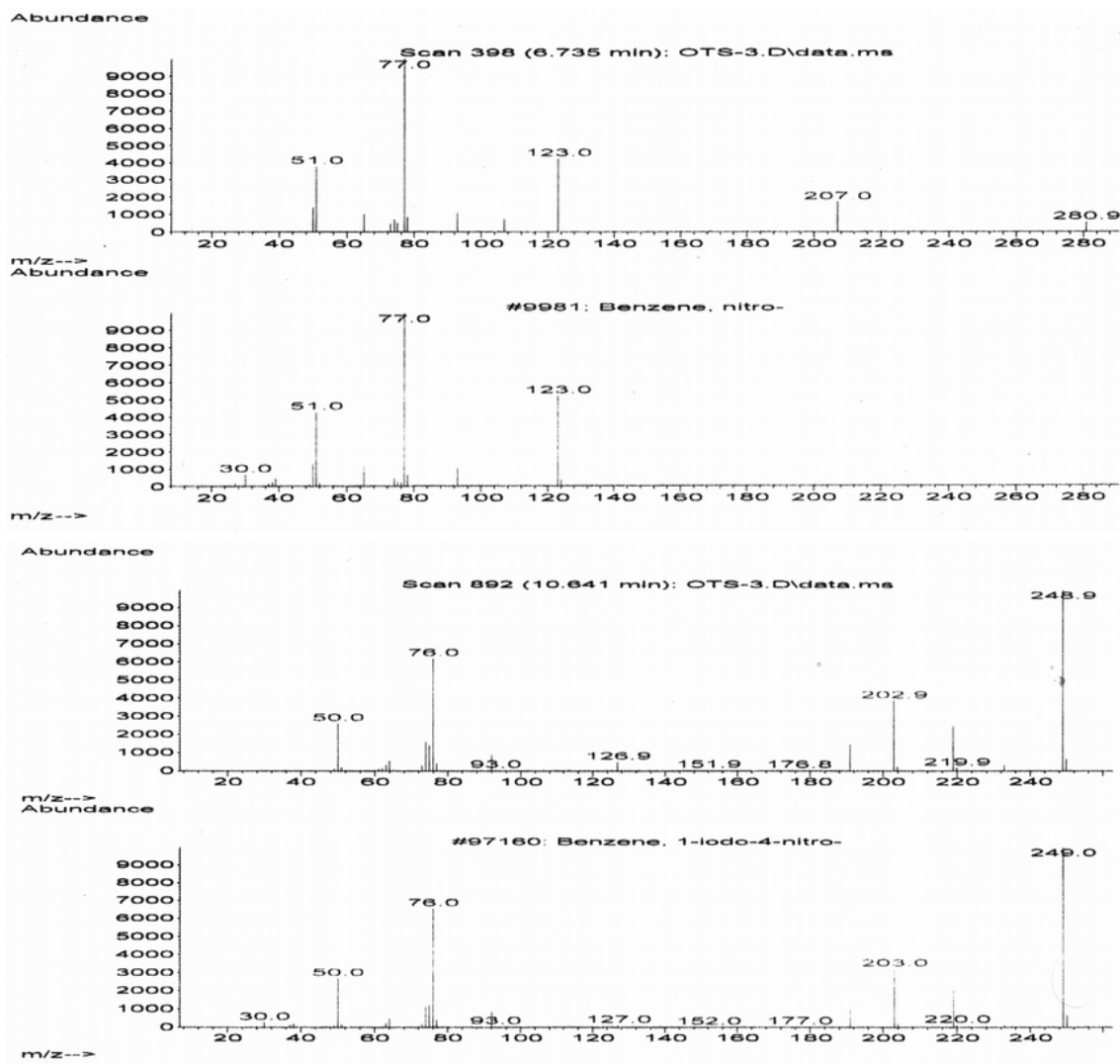
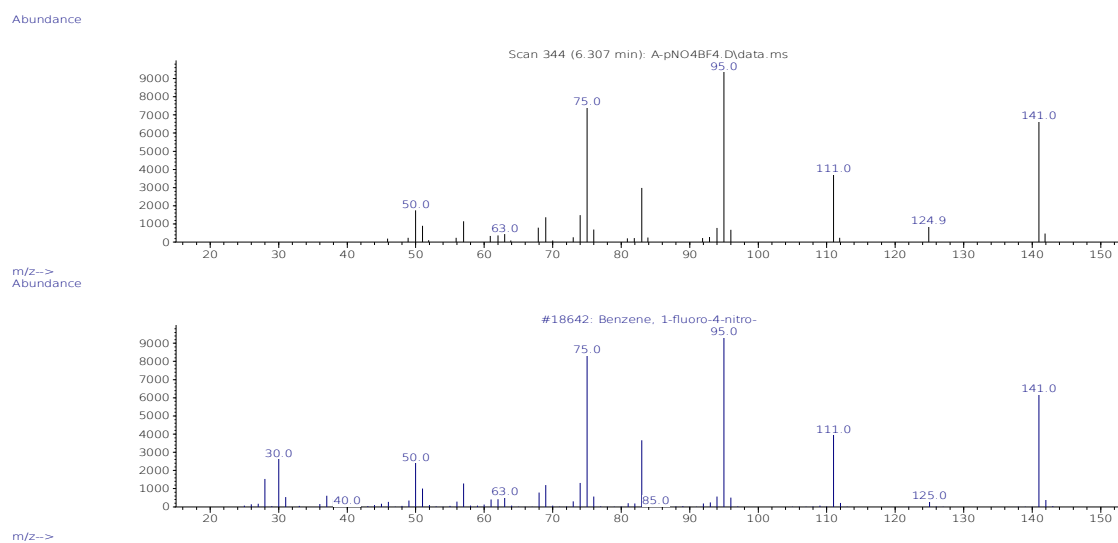


Figure 24. The major products of decomposition of DS 2 according to GC-MS data. Fragmentation patterns correspond to nitrobenzene M/Z: 123, 77, 51 and 1-iodo-4-nitrobenzene M/Z: 249, 203, 76, 50.



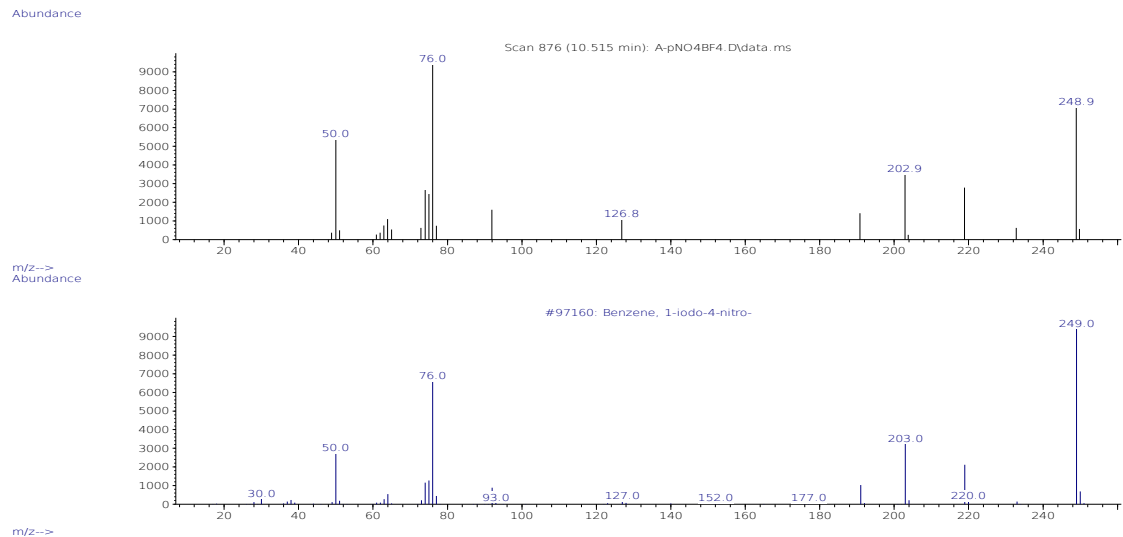


Figure 25. The major products of decomposition of DS 3 according to GC-MS data. Fragmentation patterns correspond to 1-fluoro-2-nitrobenzene M/Z: 141, 111, 95, 75, 50 and 1-iodo-4-nitrobenzene M/Z: 249, 203, 76.

### **Supporting 3s. LS-MS spectra of the decomposition products of diazonium salts studied**

The acquired LS-MS spectra can be found in [Supporting/LC-MS](#). To view and analyze the data the free OpenMS software can be used (<https://www.openms.de/>).

### **Supporting 4s. Results of quantum-chemical calculations**

The .out files for quantum chemical calculations can be found in [Supporting/Quant/Out](#). The files containing structures with optimized geometries are given in [Supporting/Quant/Mol](#).